Supporting Information

Stereochemical Effects on the Mechanical and Viscoelastic Properties of Renewable Polyurethanes Derived from Isohexides and Hydroxymethylfurfural

Robert J. Kieber III, Samantha A. Silver, and Justin G. Kennemur[a]*

[a] Department of Chemistry and Biochemistry, Florida State University, Tallahassee, FL 32303 USA

Table of Contents:

Scheme S1: Synthesis of ISBIP.

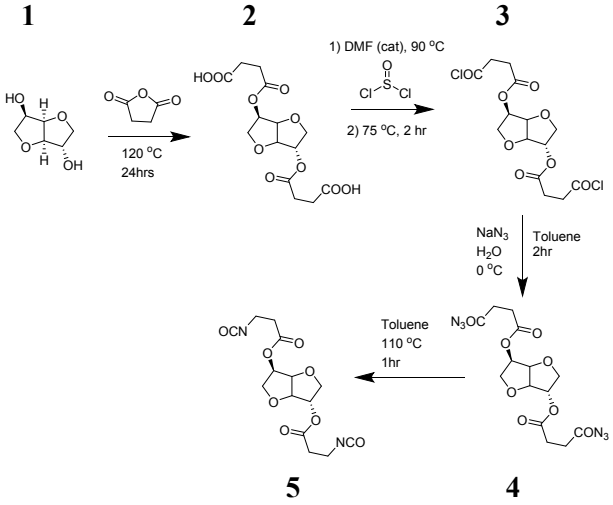

Scheme S2: Synthesis IMBIP.

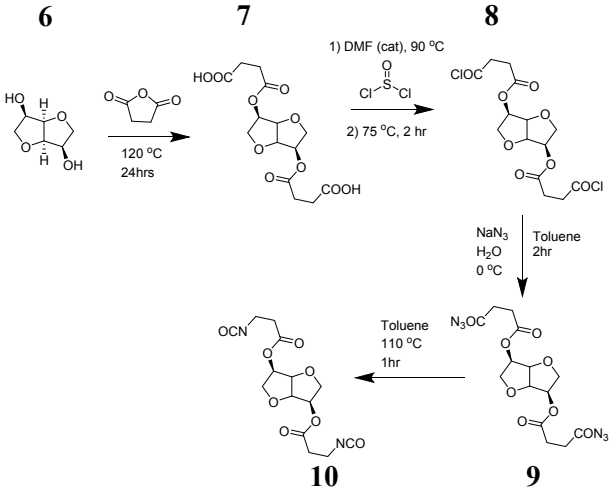

Scheme S3: Synthesis of BHMF

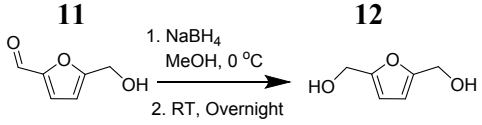

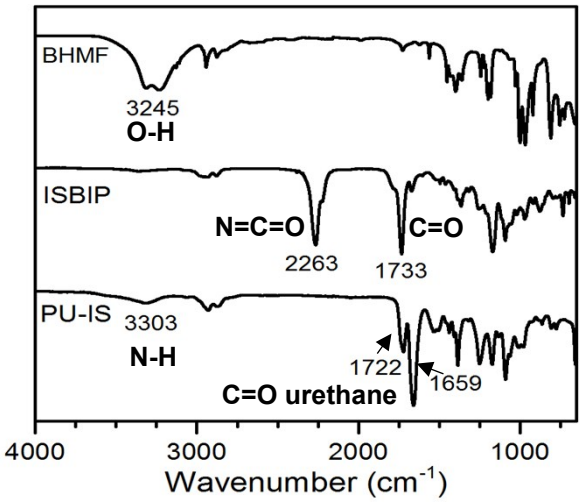

Figure S1: ATR-FTIR of BHMF, ISBIP, and an example polyurethane (PU-IS)

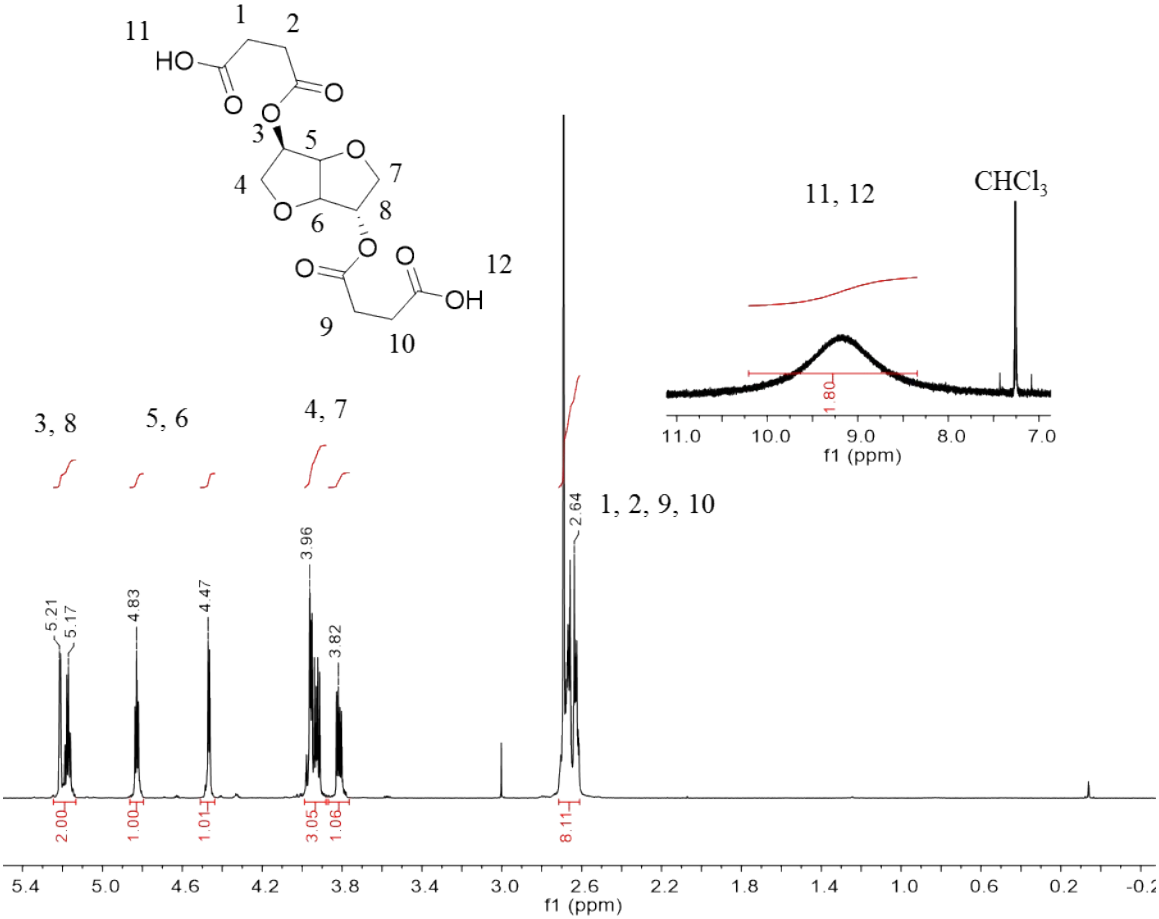

Figure S2: ^{1}H NMR of Isosorbide Extended Carboxylic Acid (**2**). Inset shows COOH peak (600 MHz, Chloroform-*d*)

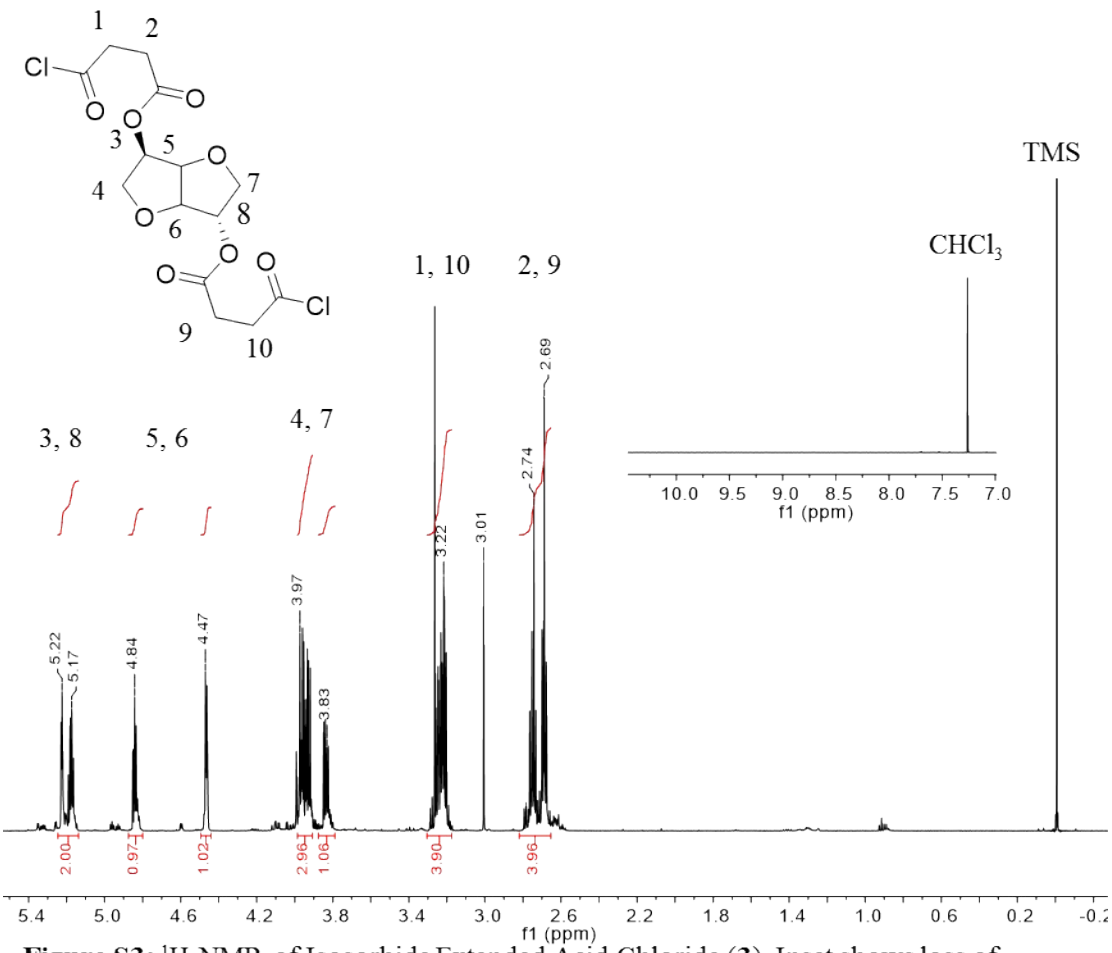

Figure S3: ^{1}H NMR of Isosorbide Extended Acid Chloride (**3**). Inset shows loss of COOH peak (600 MHz, Chloroform-*d*)

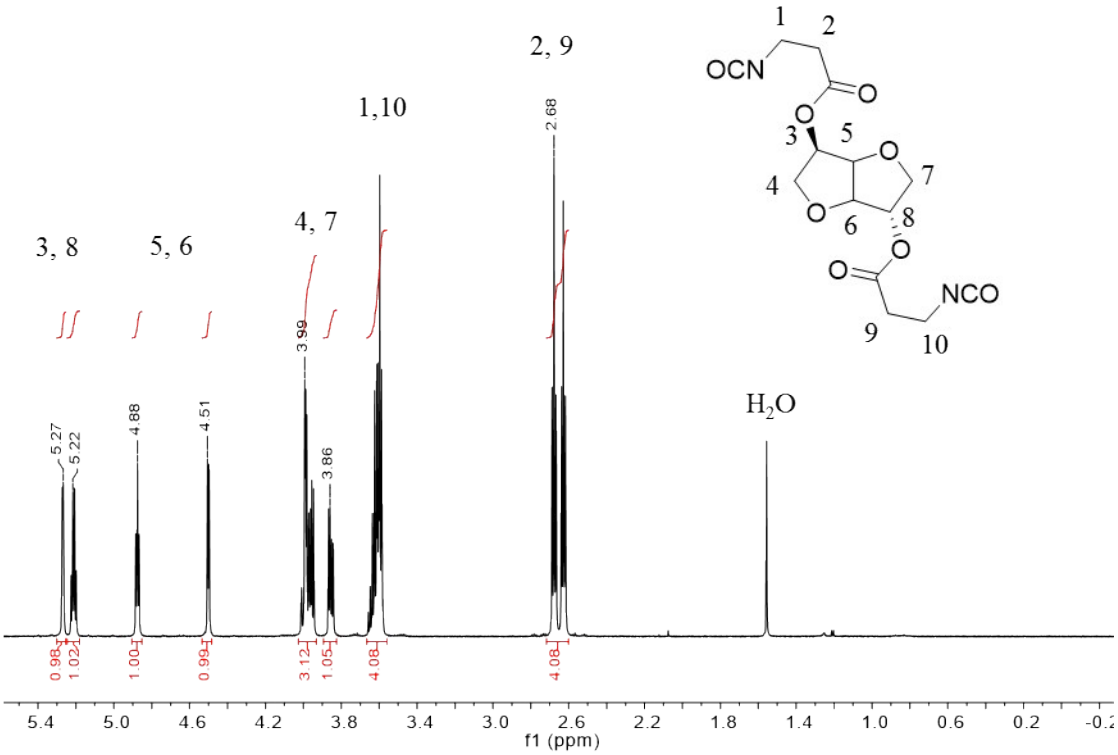

Figure S4: ^{1}H NMR of ISBIP (**5**) (600 MHz, Chloroform-*d*)

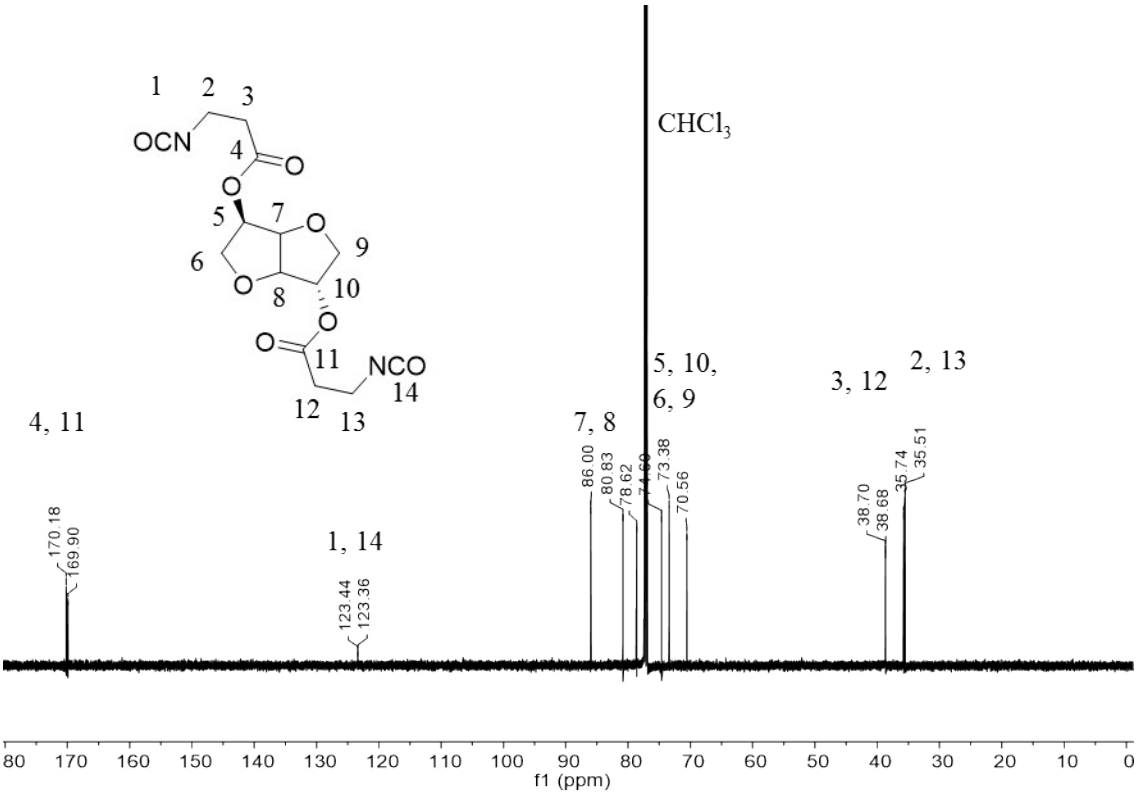

Figure S5: ^{13}C NMR of ISBIP (**5**) (151 MHz, Chloroform-*d*)

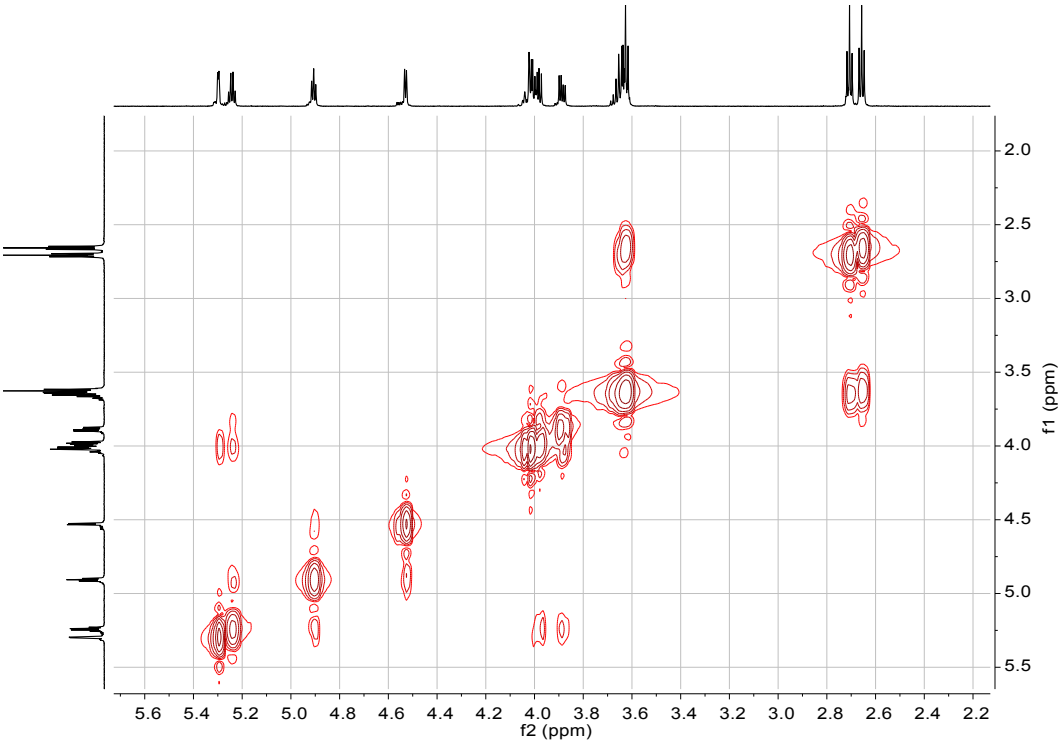

Figure S6: COSY ISBIP(**5**) (600 MHz, 25 °C, chloroform-*d*)

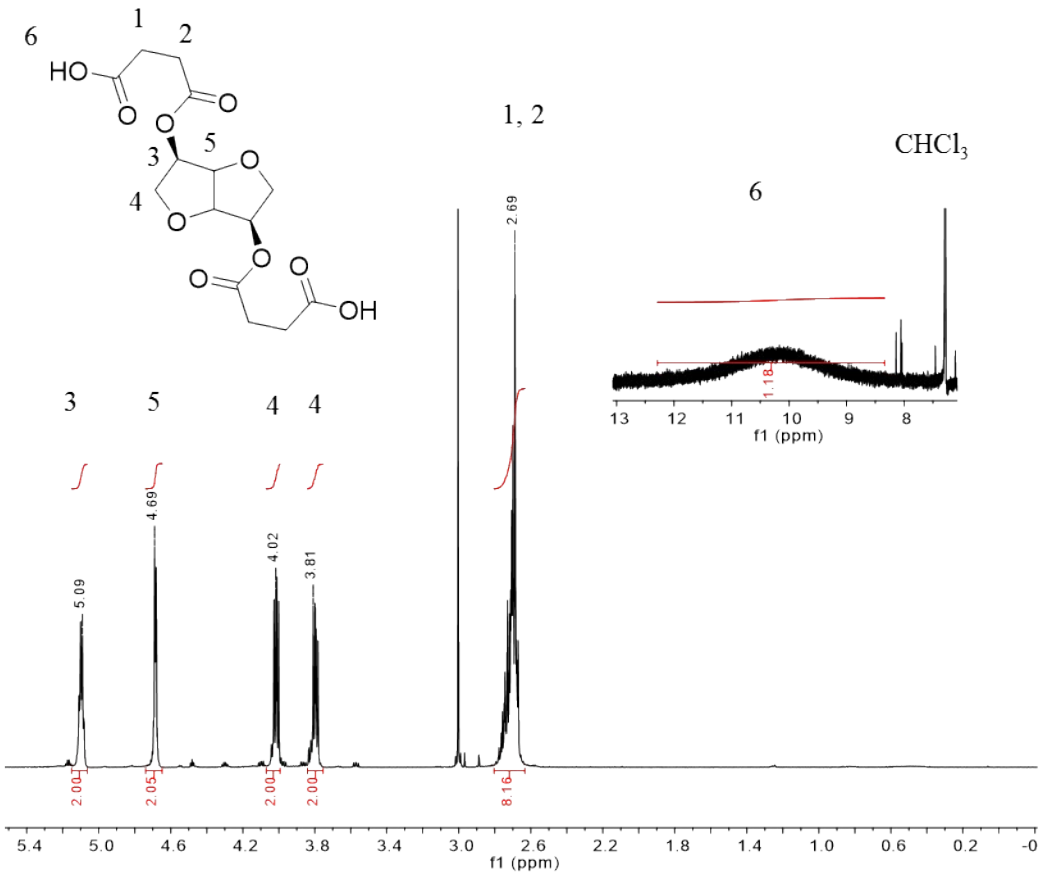

Figure S7: ^{1}H NMR of Isomannide Extended Carboxylic Acid (**7**). Inset shows COOH peak (600 MHz, Chloroform-*d*)

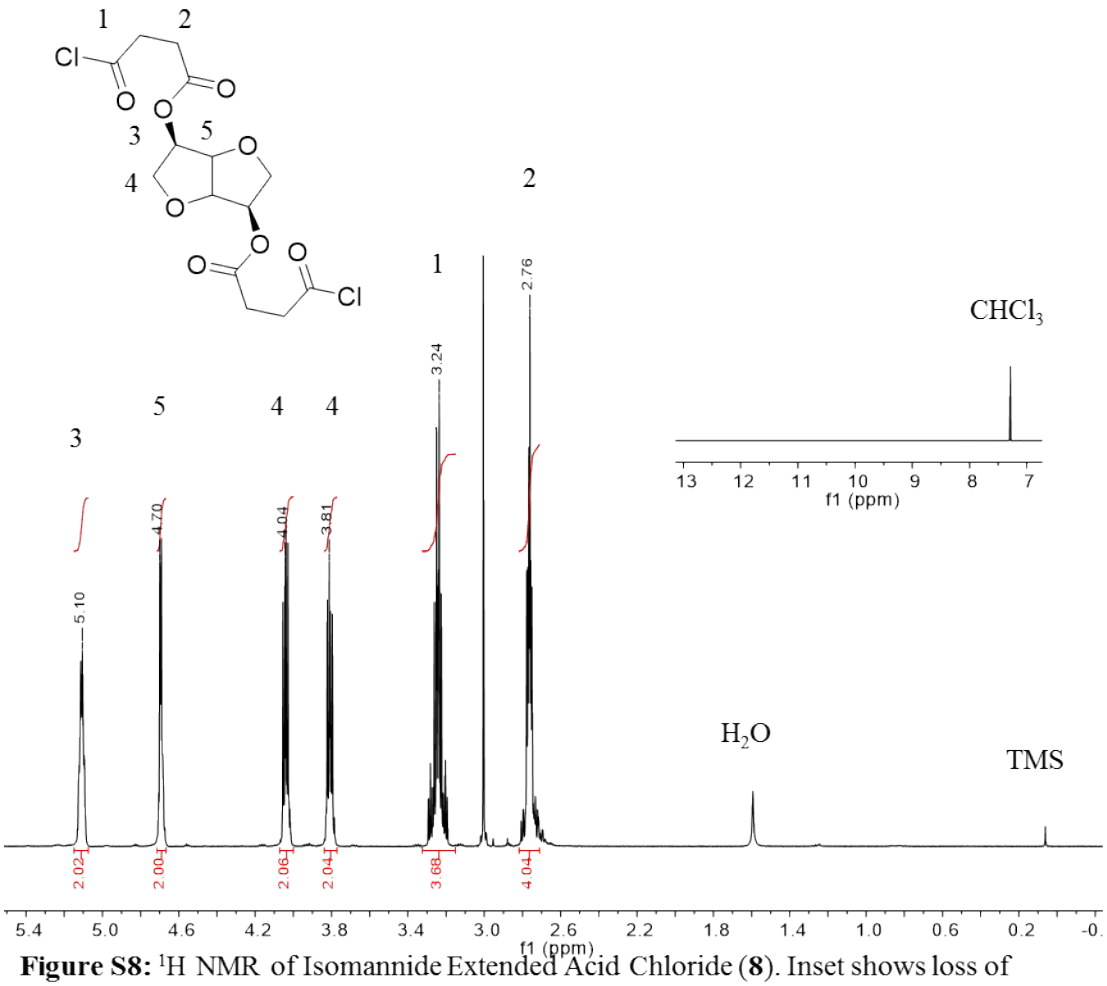

Figure S8: ^{1}H NMR of Isomannide Extended Acid Chloride (**8**). Inset shows loss of COOH peak (600 MHz, Chloroform-*d*)

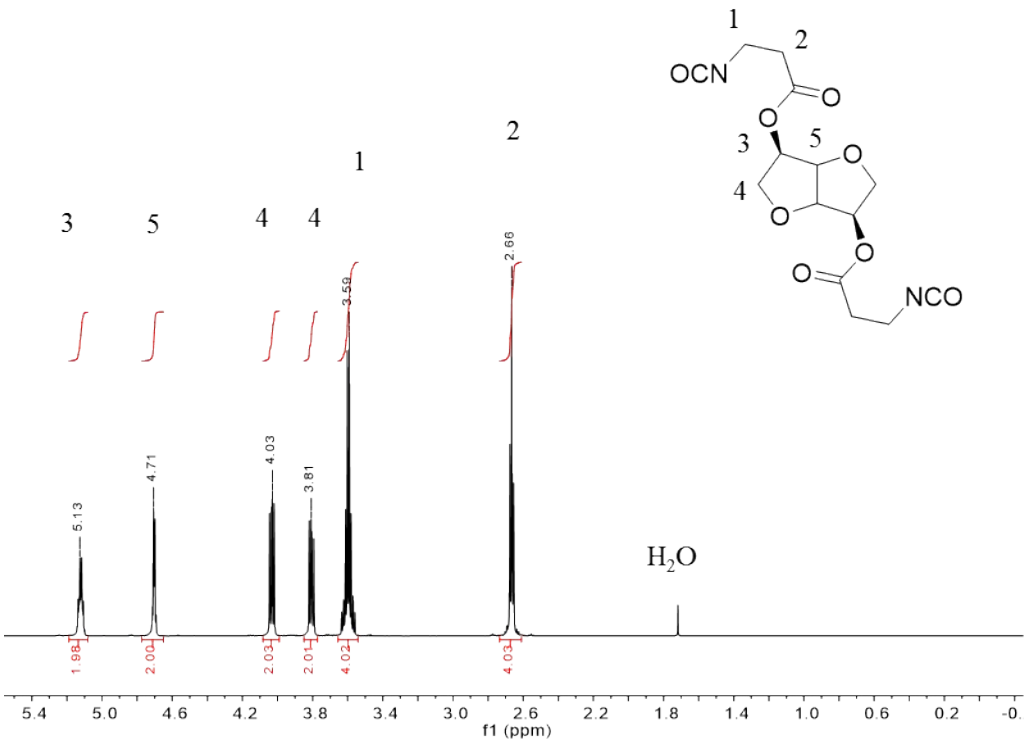

Figure S9: ^{1}H NMR of IMBIP (**10**) (600 MHz, Chloroform-*d*)

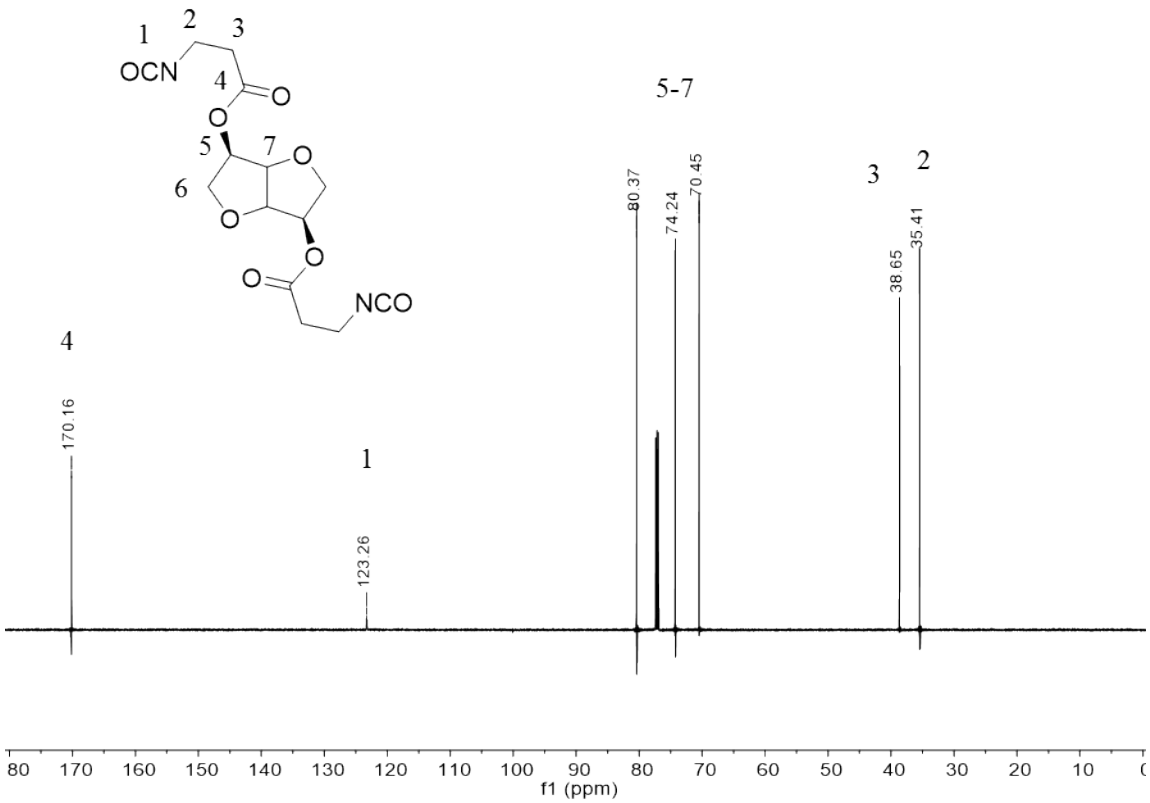

Figure S10: ^{13}C NMR of IMBIP (**10**) (151 MHz, Chloroform-*d*)

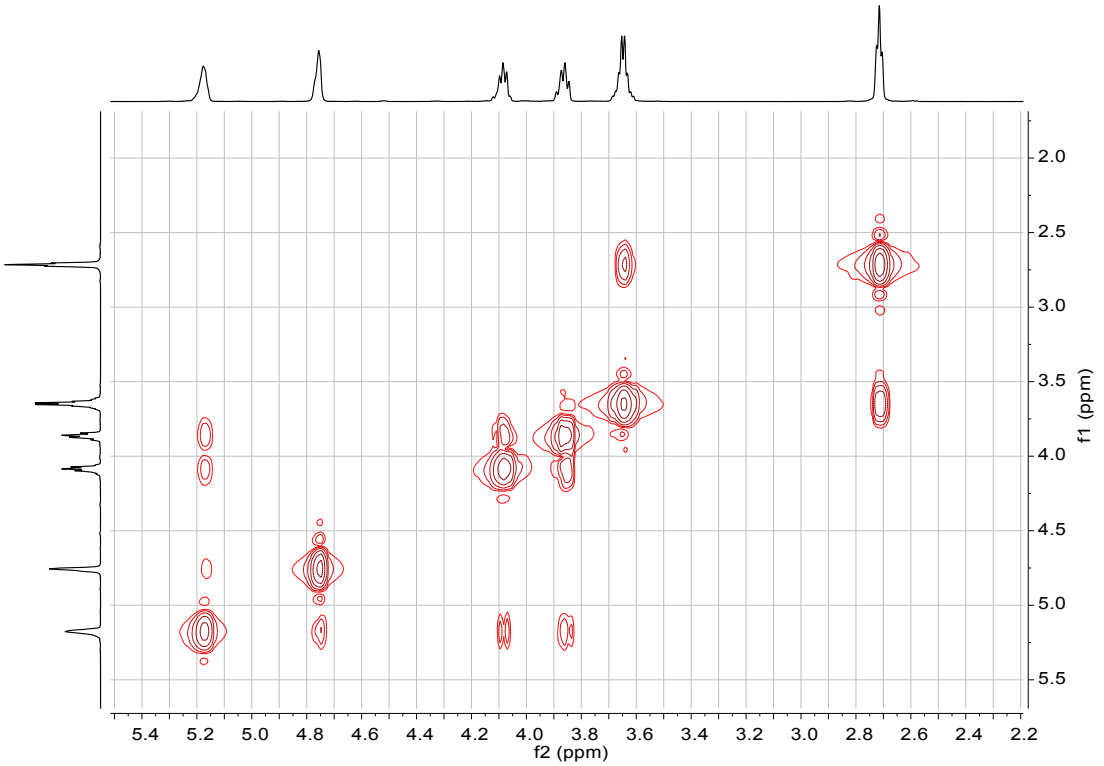

Figure S11: COSY IMBIP (**10**) (600 MHz, 25 °C, chloroform-*d*)

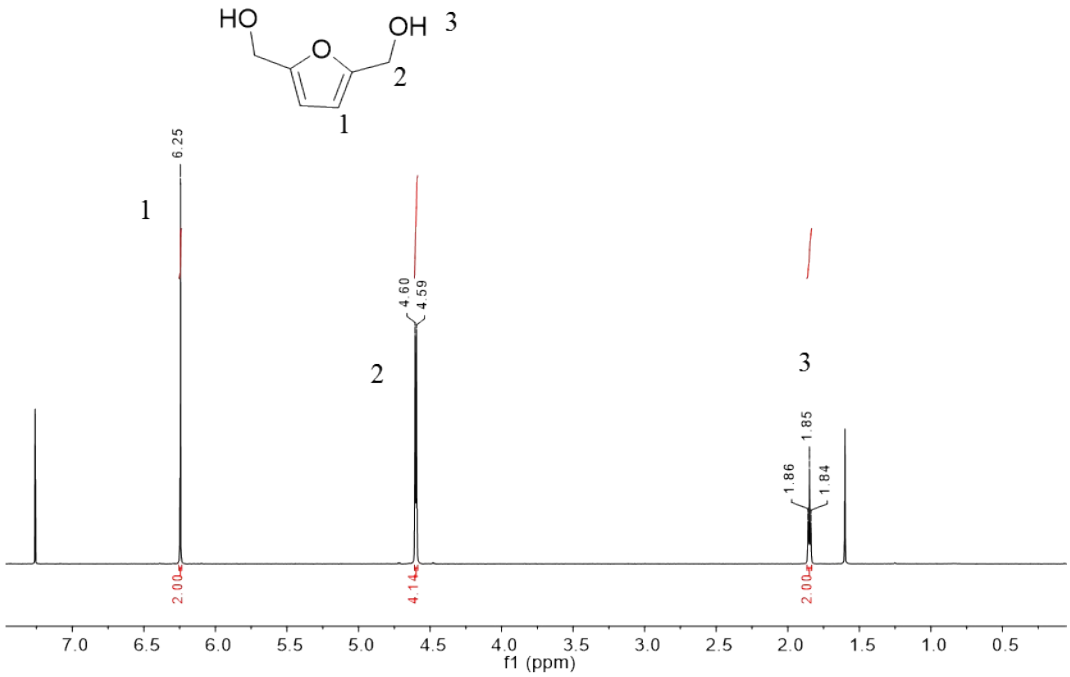

Figure S12: ^{1}H NMR of BHMF (**12**) (600 MHz, Chloroform-*d*)

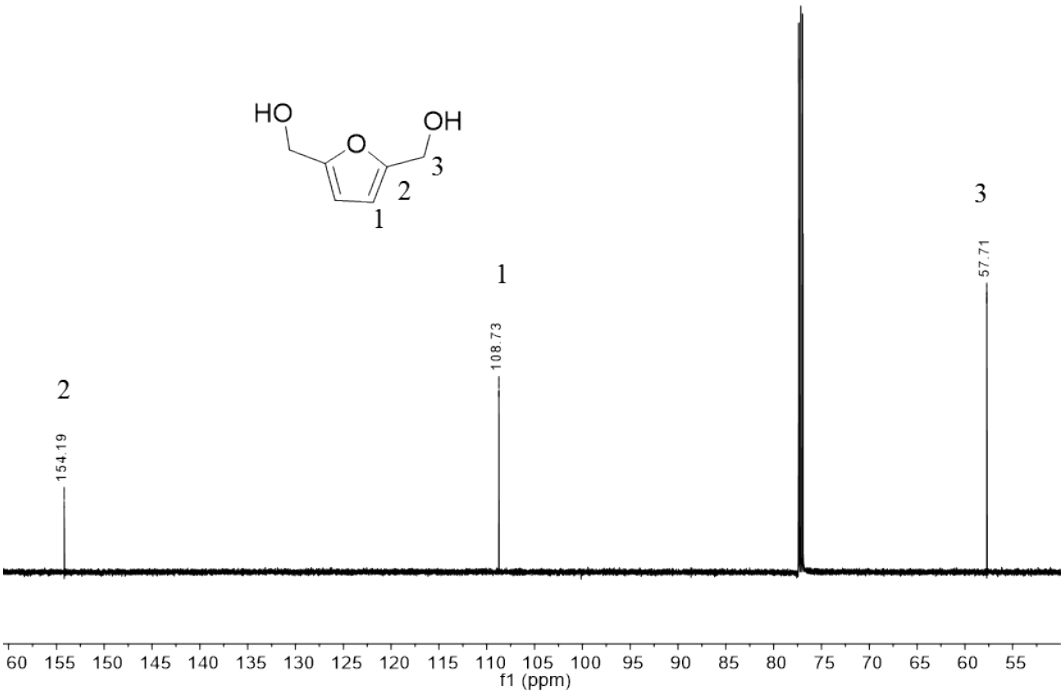

Figure S13: ^{13}C NMR of BHMF (**12**) (151 MHz, Chloroform-*d*)

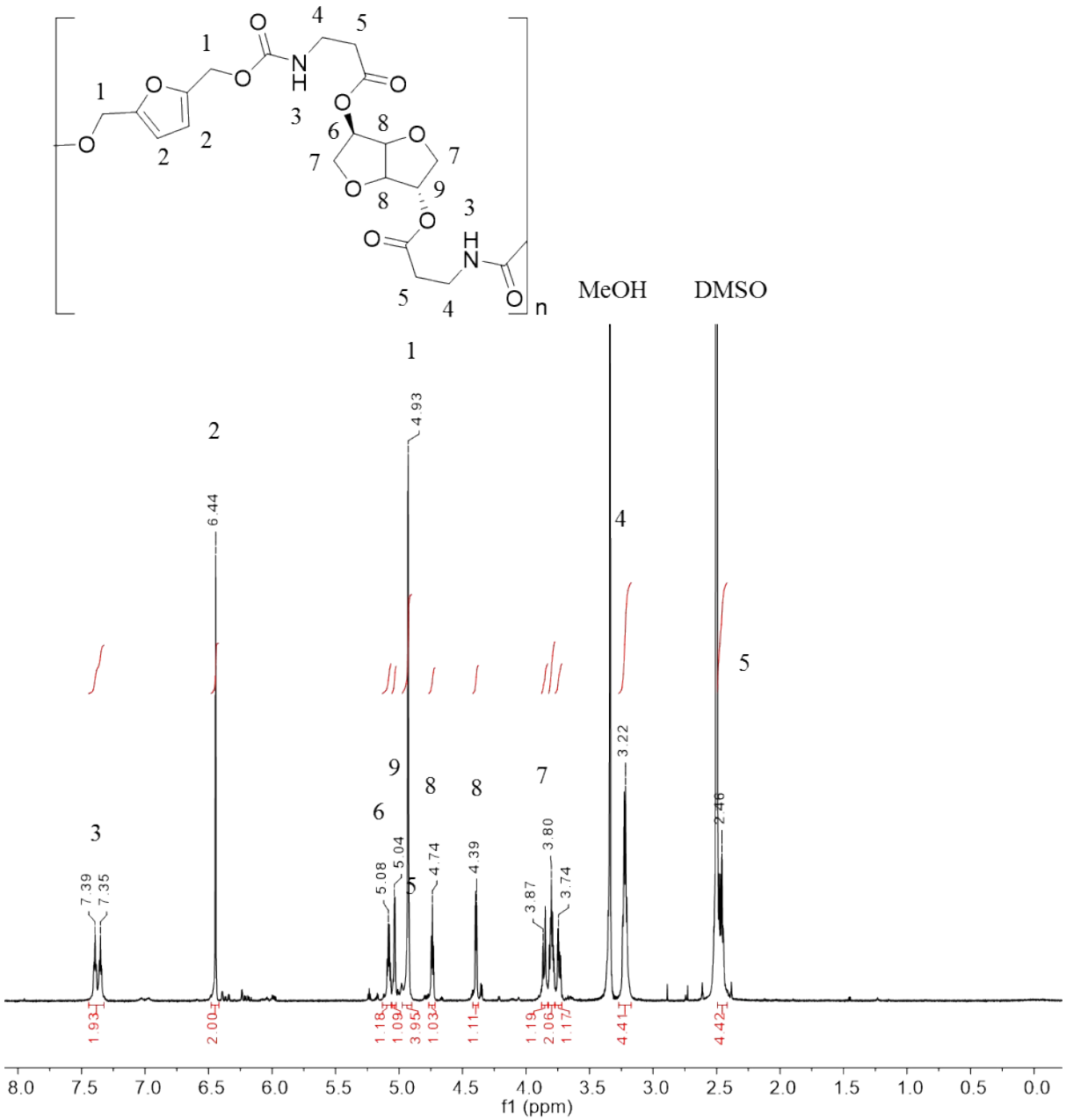

Figure S14: ^{1}H NMR of PU-IS (600 MHz, DMSO-d_6)

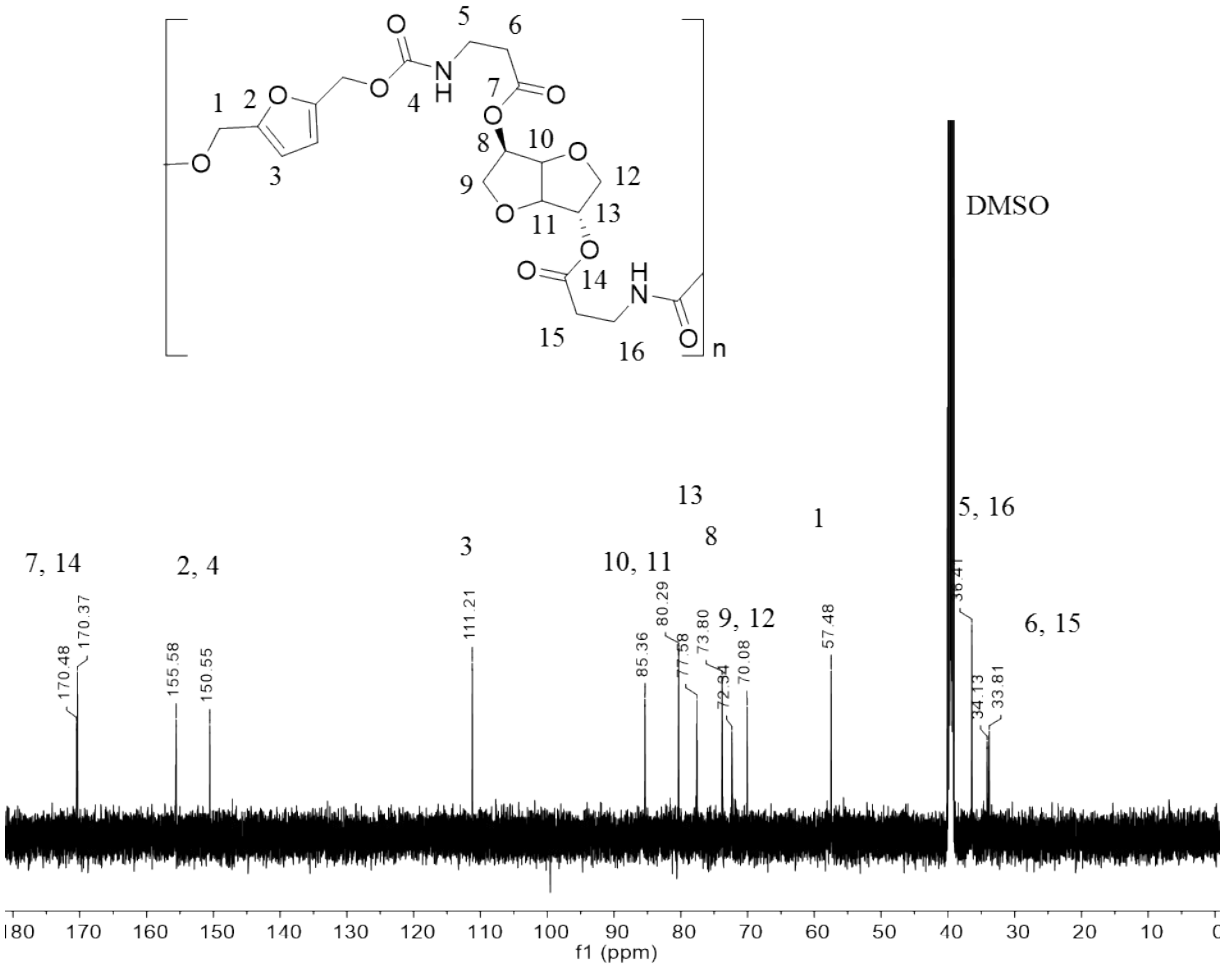

Figure S15: ^{13}C NMR of PU-IS (600 MHz, DMSO-d_6)

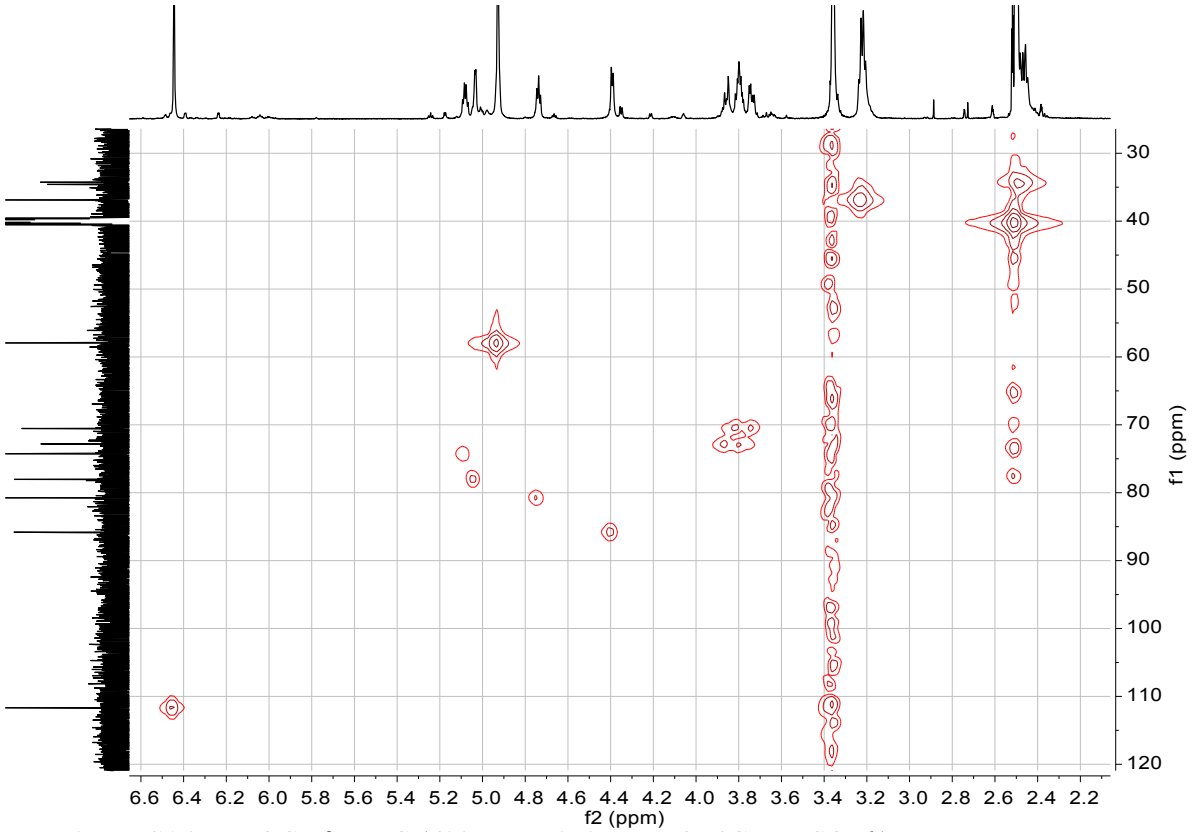

Figure S16: HMQC of PU-IS (600 MHz, 150 MHz, 25 °C, DMSO-d_6)

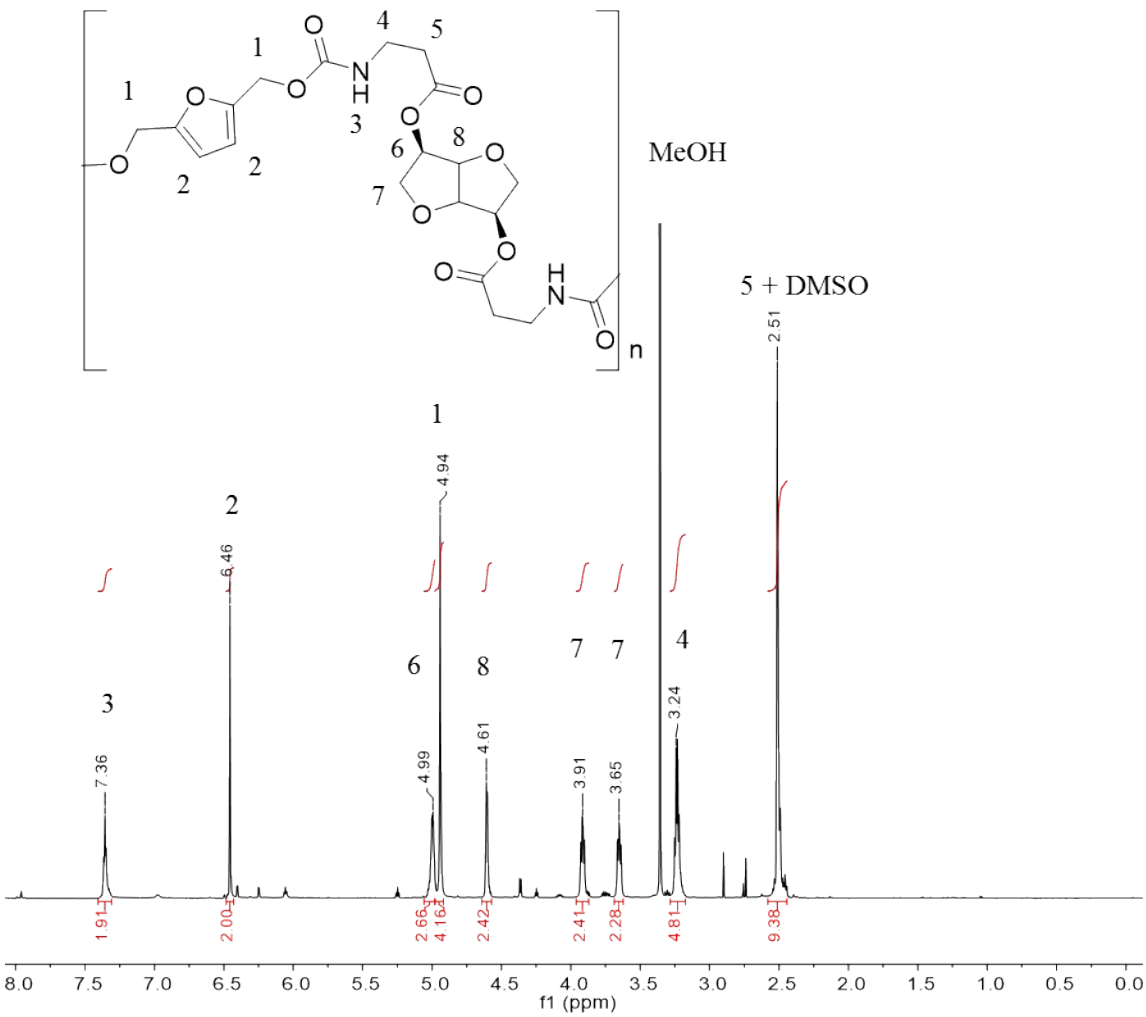

Figure S17: ^{1}H NMR of PU-IM (600 MHz, DMSO-d_6)

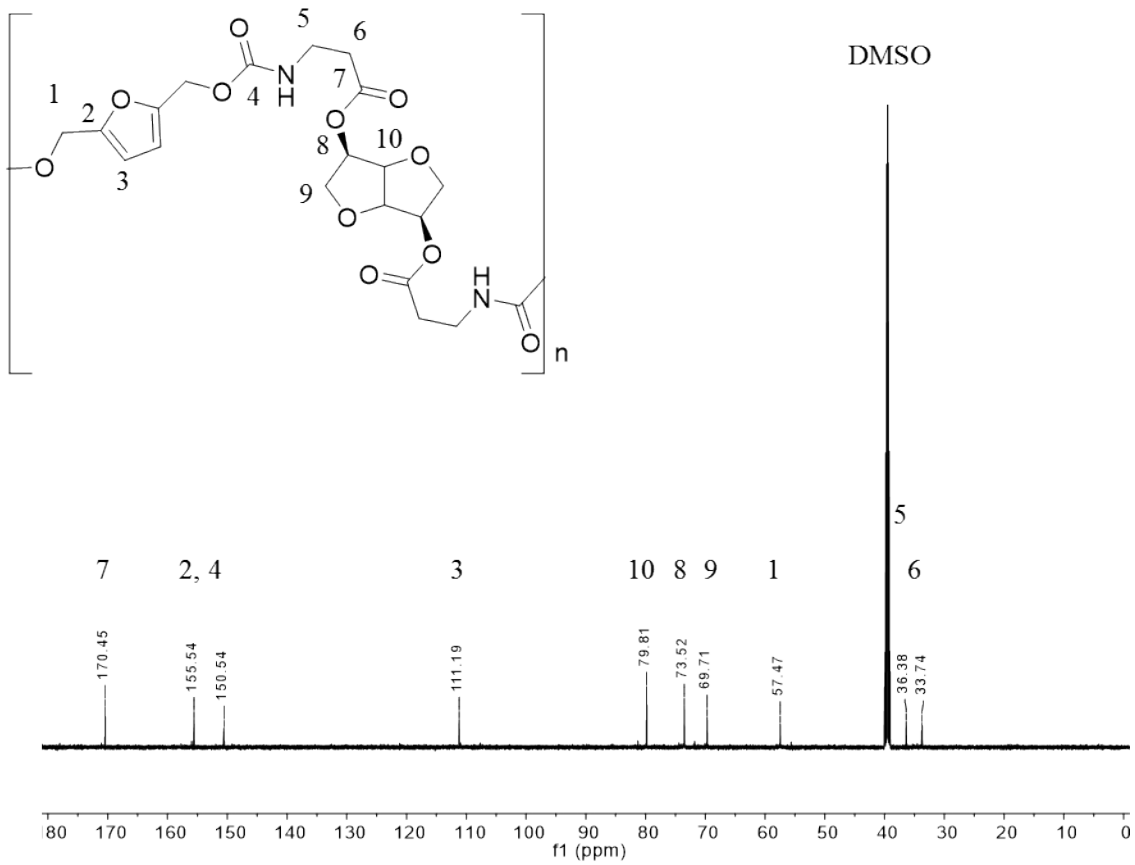

Figure S18: ^{13}C NMR of PU-IM (151 MHz, DMSO-d_6)

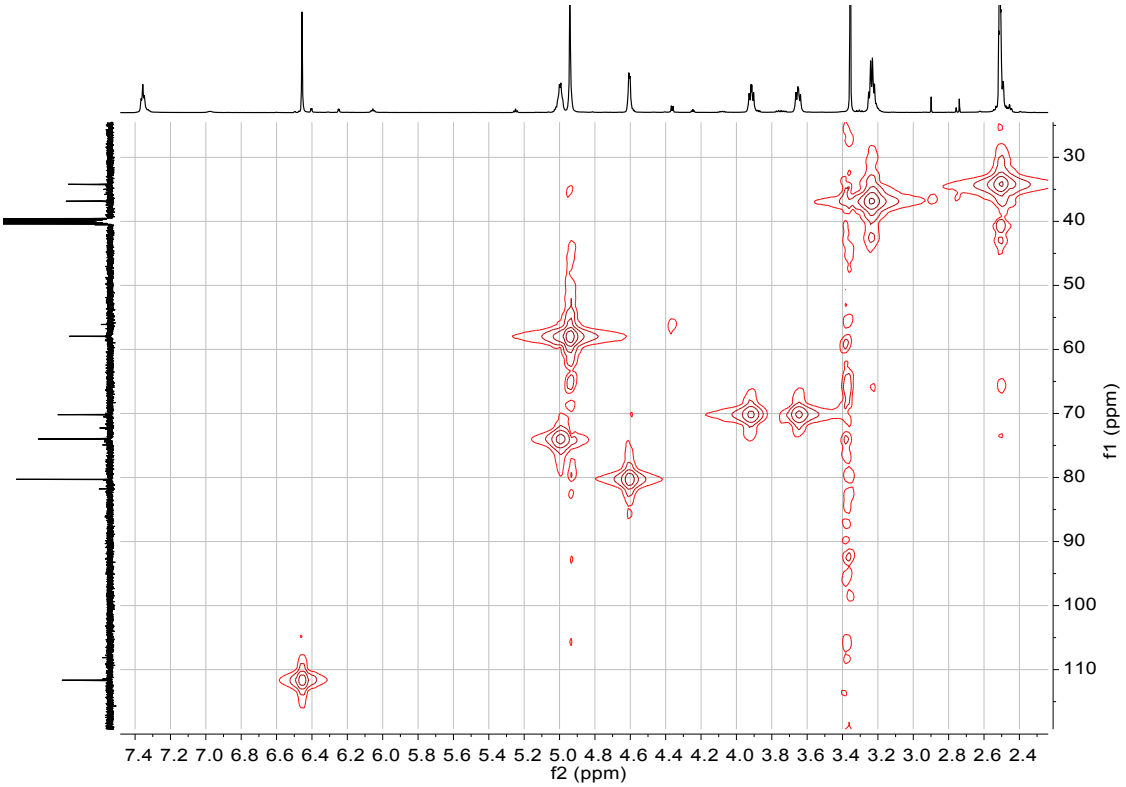

Figure S19: HMQC PU-IM (600 MHz, 150 MHz, DMSO-d_6)

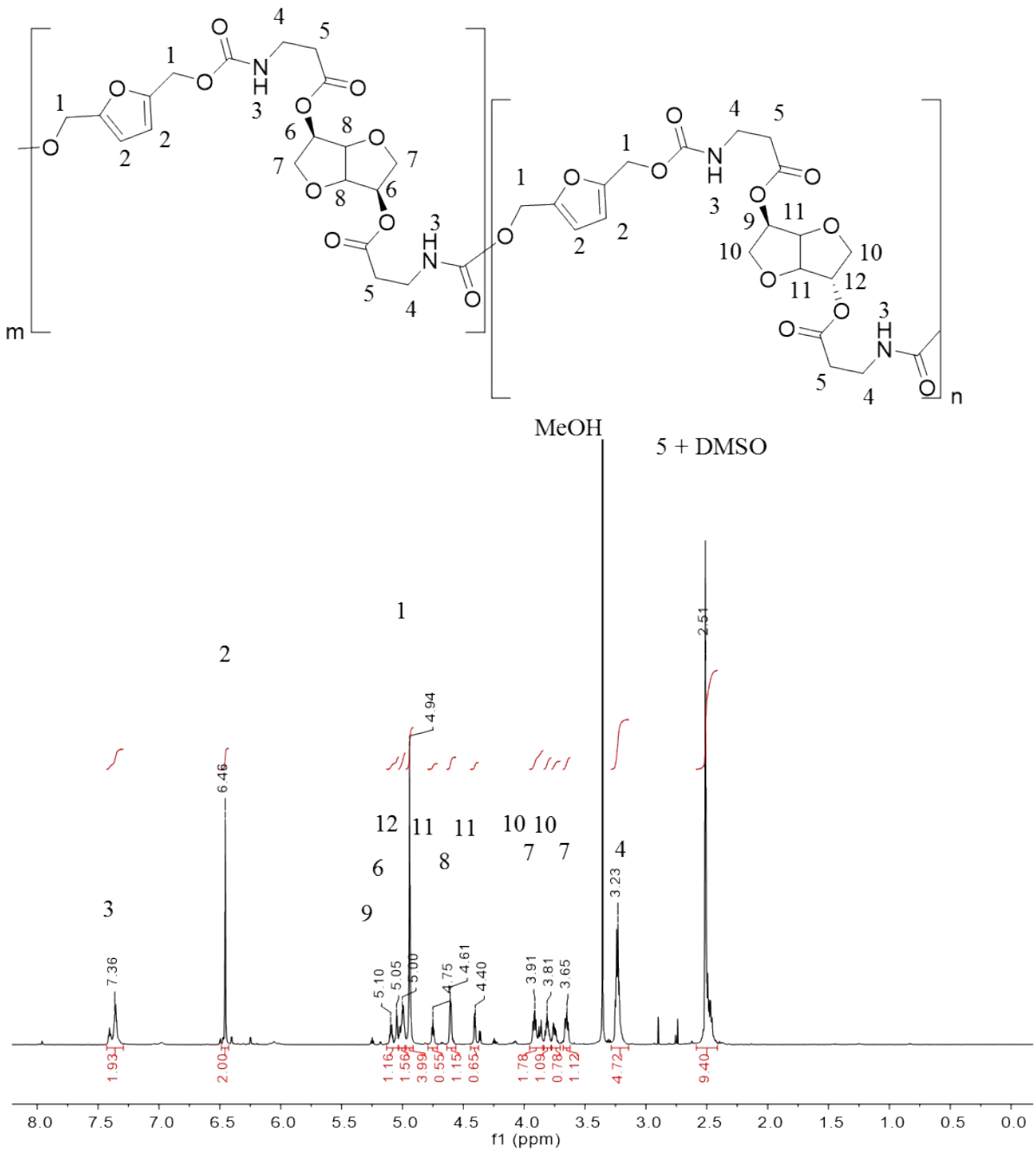

Figure S20: ^{1}H NMR PU-IS$_{0.5}$IM$_{0.5}$ (600 MHz, DMSO-d_6).

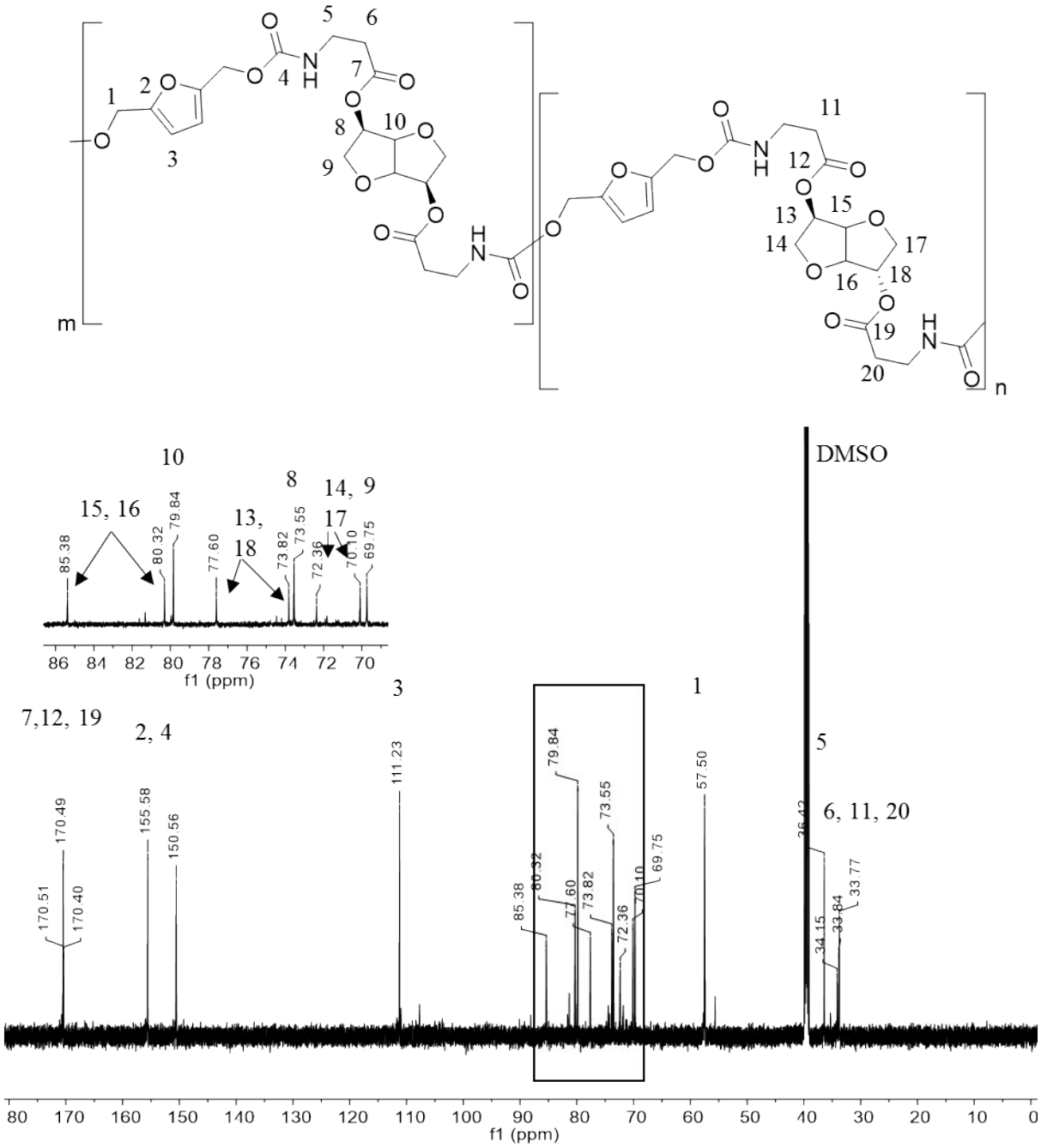

Figure S21: ^{13}C NMR PU-IS$_{0.5}$IM$_{0.5}$. Inset shows region in black box expanded. (151 MHz, DMSO-d_6)

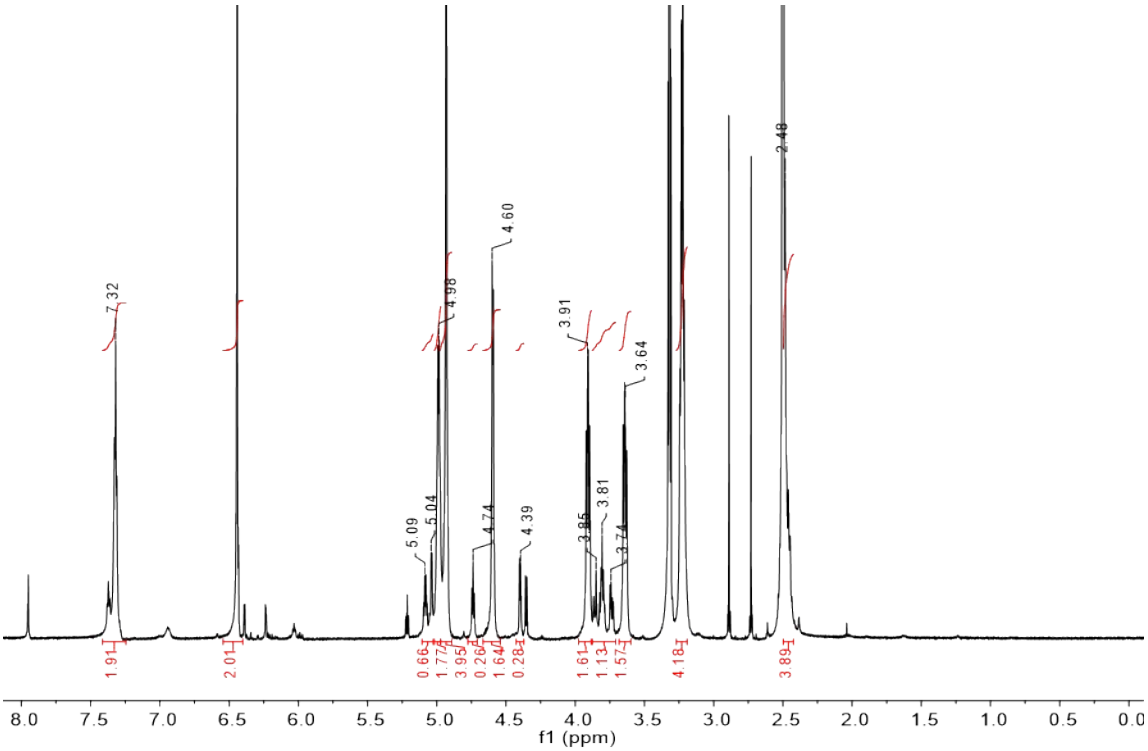

Figure S22: ^{1}H NMR PU-IS$_{0.25}$IM$_{0.75}$. (600 MHz, DMSO-d_6).

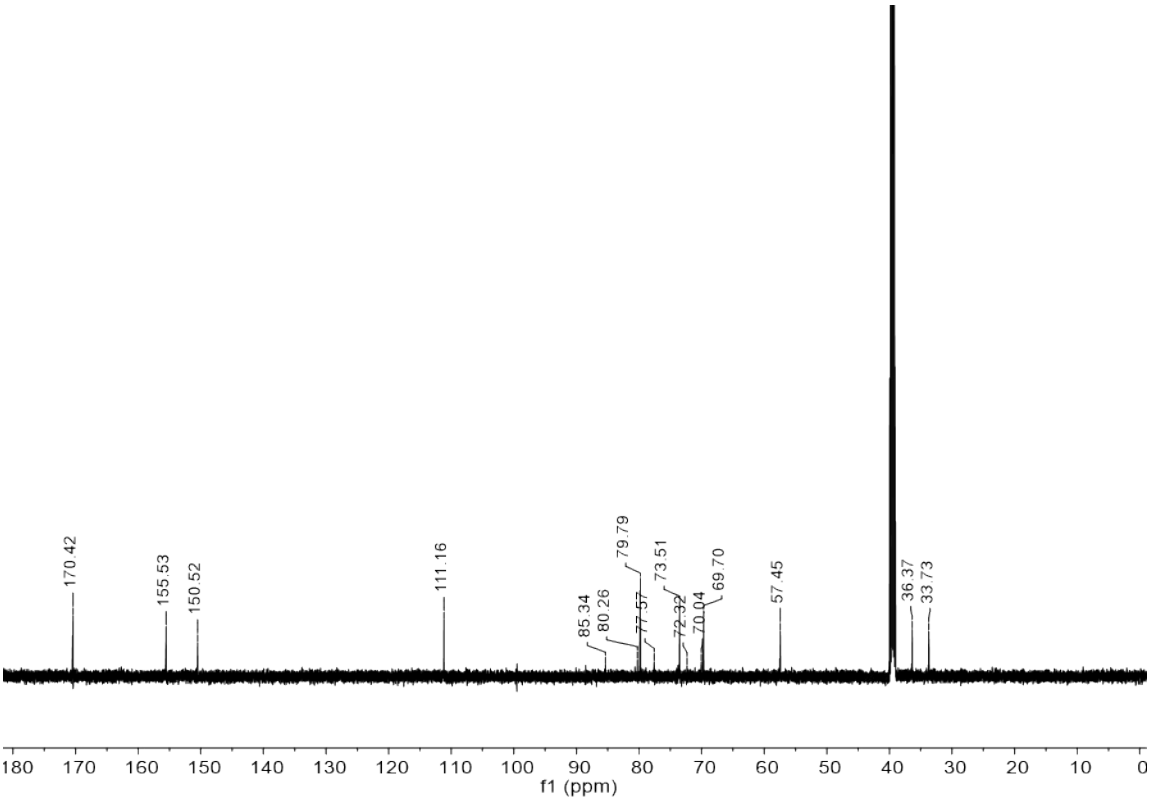

Figure S23: ^{13}C NMR PU-IS$_{0.25}$IM$_{0.75}$. (151 MHz, DMSO-d_6).

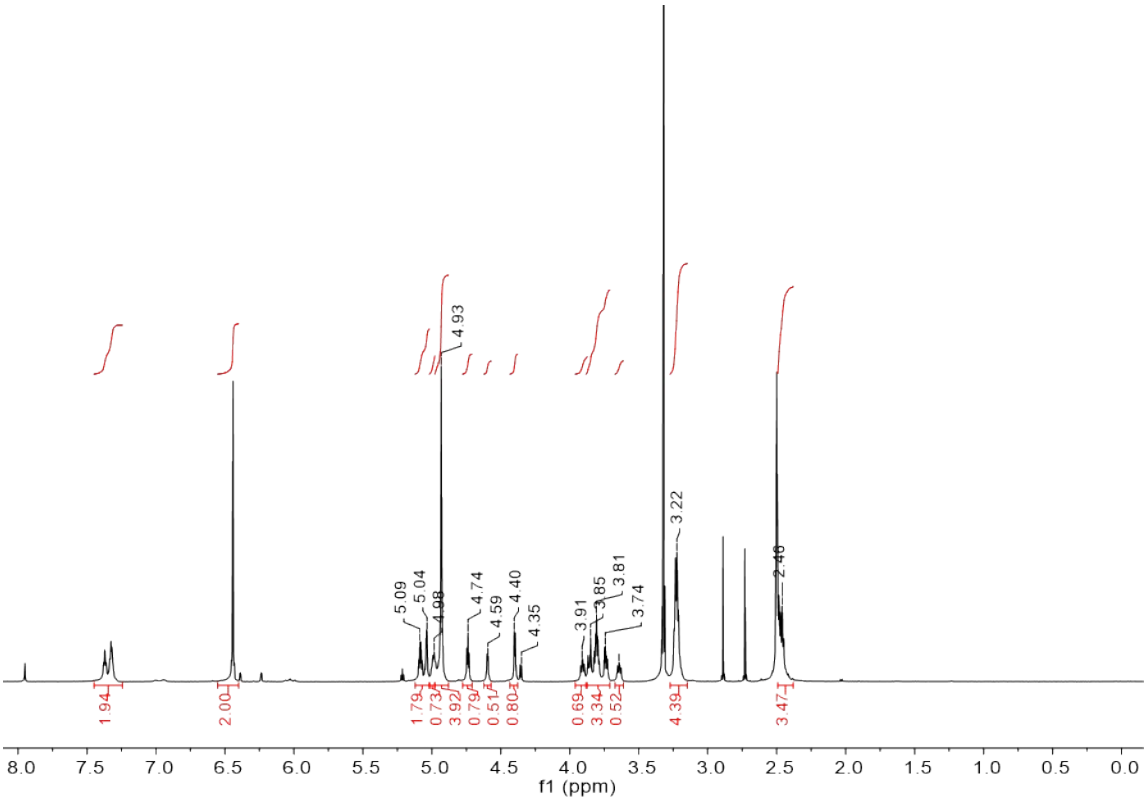

Figure S24: ^{1}H NMR PU-IS$_{0.75}$IM$_{0.25}$. (600 MHz, DMSO-d_6).

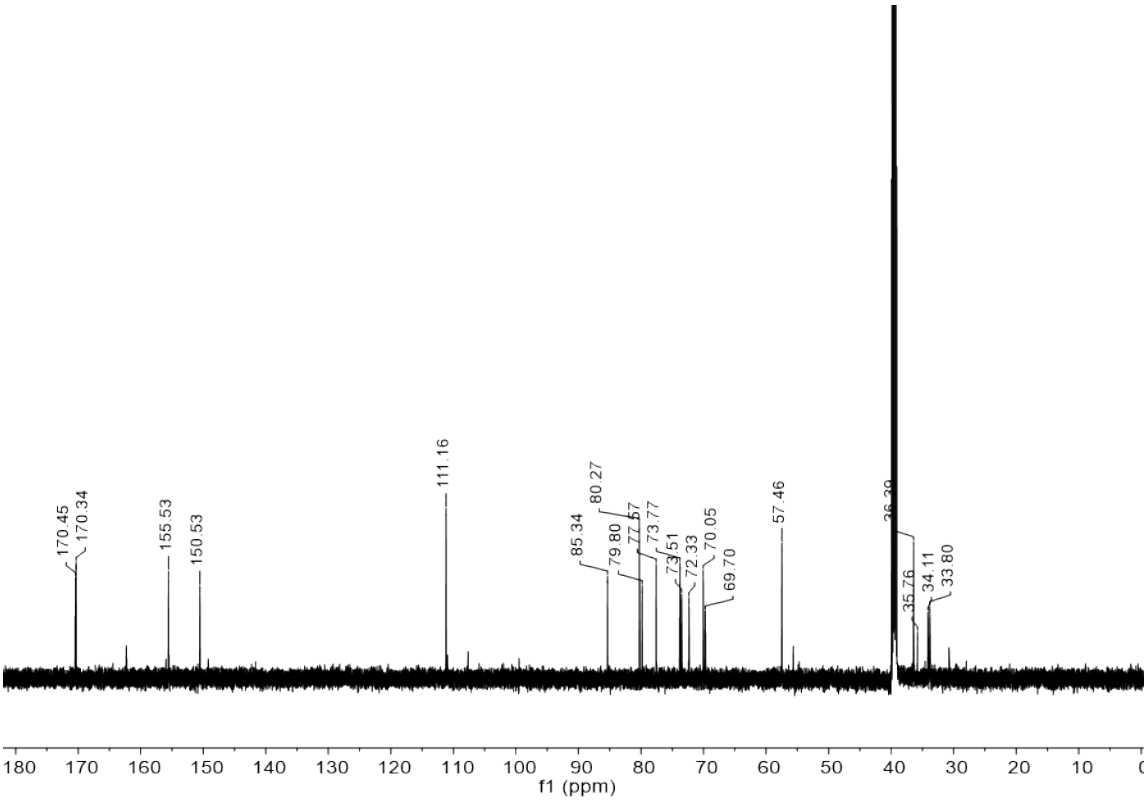

Figure S25: ^{13}C NMR PU-IS$_{0.75}$IM$_{0.25}$. (151 MHz, DMSO-d_6).

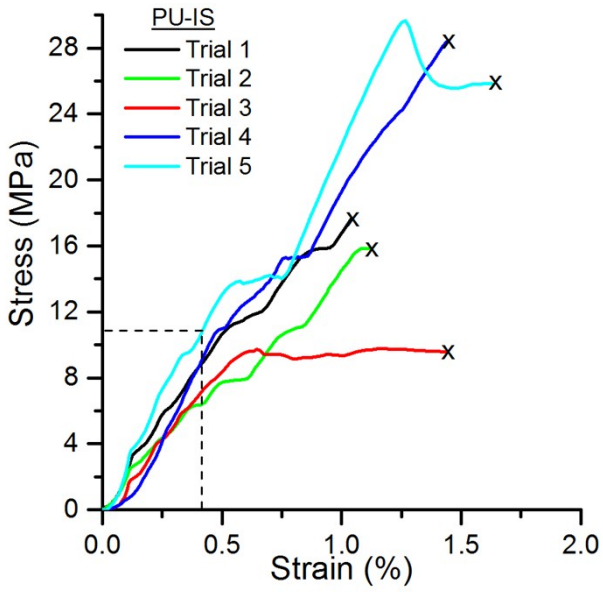

Figure S26: Stress-strain curve for sample PU-IS. Stress was applied uniaxially at a rate 50% of the original length in mm min^{-1}. Trial 4 and Trial 5 were taken as the representative toughest samples and averaged for Figure 4a. Dashed box indicates region used to calculate *E*.

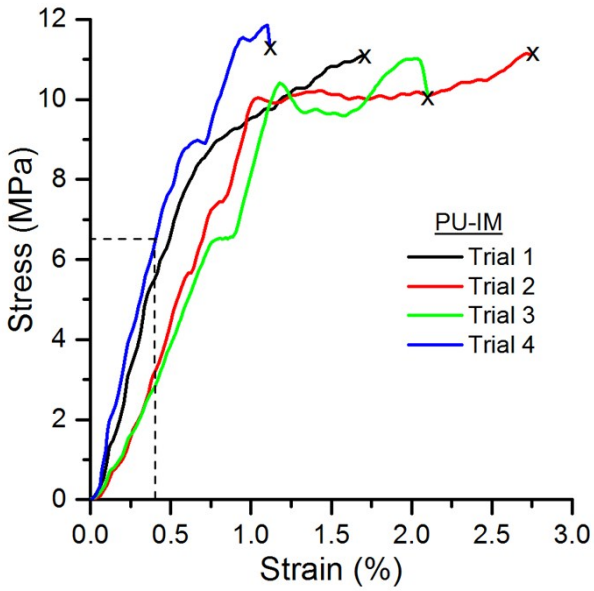

Figure S27: Stress-strain curve for sample PU-IM. Stress was applied uniaxially at a rate 50% of the original length in mm min^{-1}. Trial 1, Trial 2, and Trial 3 were taken as the representative toughest samples and averaged for Figure 4. Dashed box indicates region used to calculate *E*.

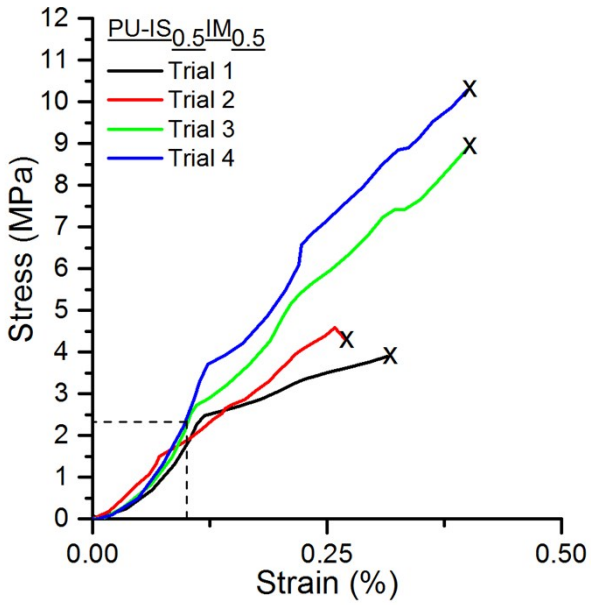

Figure S28: Stress-strain curve for sample PU-$IS_{0.5}IM_{0.5}$. Stress was applied uniaxially at a rate 50% of the original length in mm min^{-1}. Trials 3 and 4 were used as representative toughest samples and averaged for Figure 4. Dashed box indicates region used to calculate *E*.

Equation S1: Calculation for determining dn/dc for polyurethanes with varying stereochemistry

$$\frac{dn}{dc} = \left(\frac{dn}{dc} pure\ IS\right)(X_{IS}) + \left(\frac{dn}{dc} pure\ IM\right)(X_{IM})$$

Equation S2: Williams-Landel-Ferry (WLF) equation relating frequency factor (a_T) (Table S1) to T, using a reference temperature T_r of 120 ºC.

$$\log(a_T) = -\frac{C_1(T - T_r)}{C_2 + (T - T_r)}$$

Equation S3: In order to determine C_1 and C_2, the WLF equation was modified to the following linear fit of $-\log(a_T)^{-1}$ vs $(T - T_r)^{-1}$, where the C_1 = 1/y-intercept and $C_2 = C_1$ * slope

$$-\frac{1}{\log(a_T)} = \frac{C_2}{C_1}\left(\frac{1}{T - T_r}\right) + \frac{1}{C_1}$$

Equation S4: Calculation of molecular weight between entanglements (M_e) using the density (ρ), the plateu modulus (G_N°) (taken as the storage modulus (G') when tan δ reaches a minimum along the ω axis), the universal gas constant R = 8.314 J mol^{-1} K^{-1}, and the reference temperature T_{ref} = 120 ºC.

$$M_e = \frac{\rho RT}{G_N^o}$$

Density determined at 23 ± 1 °C was adjusted to that predicted at 120 °C following the procedure outlined by Van Krevelen[1-2], the steps are outlined in Equations S5-S7.

Equation S5: Density of a polymer (ρ) at a given temperature T, where M_o = molecular weight of the repeat unit and $V(T)$ is the molar volume occupied at a given temperature

$$\rho(T) = \frac{M_o}{V(T)}$$

Equation S6: Calculation of the van der Waals volume (V_W)

$$V_W = \frac{V(23\ ^oC)}{1.6}$$

Equation S7: Molar volume at a given temperature T, where $T = T_{ref}$ (120 ºC)

$$V(T) = V(23\ ^oC) + 0.45 * 10^{-3}(T_g - 23\ ^oC)V_W + 1.0 * 10^{-3}(T - T_g)V_W$$

Table S2: Parameters used to calculate PU density at 120 ºC in Equation S5-S7. Densities obtained were used in Equation S4.

Sample	T_g (ºC)	ρ (23 ºC) (g cm^{-3})	M_o (g mol^{-1})	V (23 ºC) (cm^3 mol^{-1})	V_W (cm^3 mol^{-1})	ρ (120 ºC) (g cm^{-3})
PU-IS	51.5	1.37	468.42	341.9124	213.6953	1.30
PU-IS$_{0.5}$IM$_{0.5}$	41.8	1.32	468.42	354.8636	221.7898	1.25
PU-IM	40.24	1.27	468.42	368.8346	230.5217	1.20

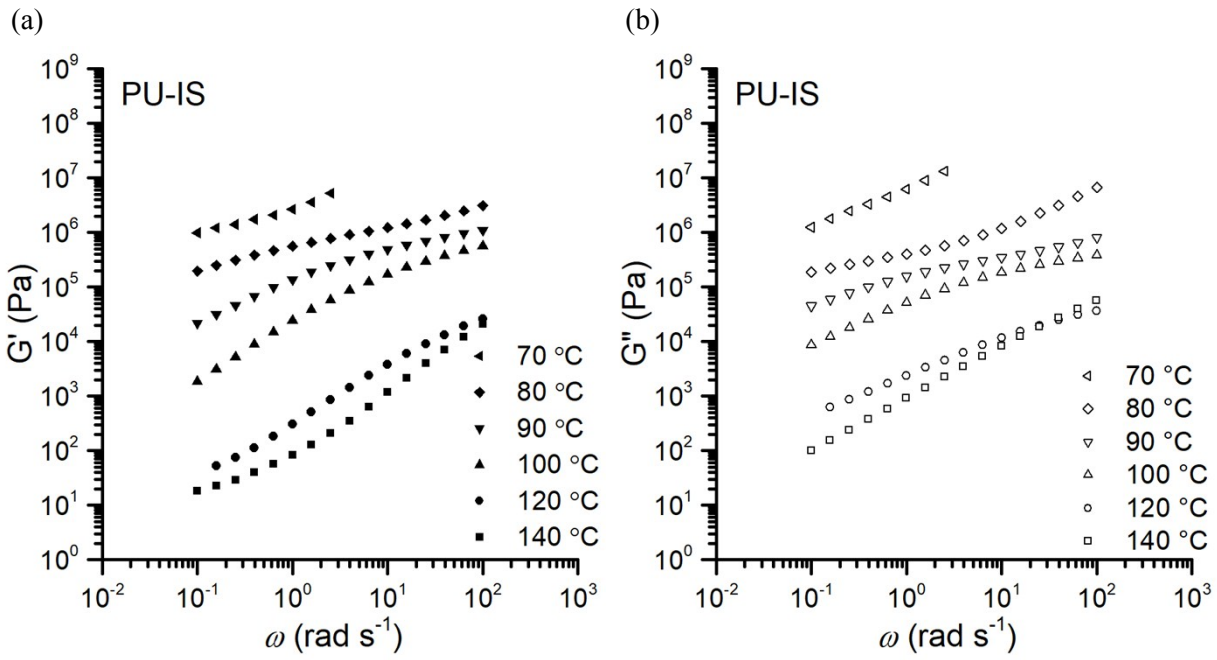

Figure S29: Frequency sweeps of (a) storage modulus (G′) and (b) loss modulus (G″) for PU-IS at varying temperature within the linear viscoelastic regime used for TTS plots in Figure 4b.

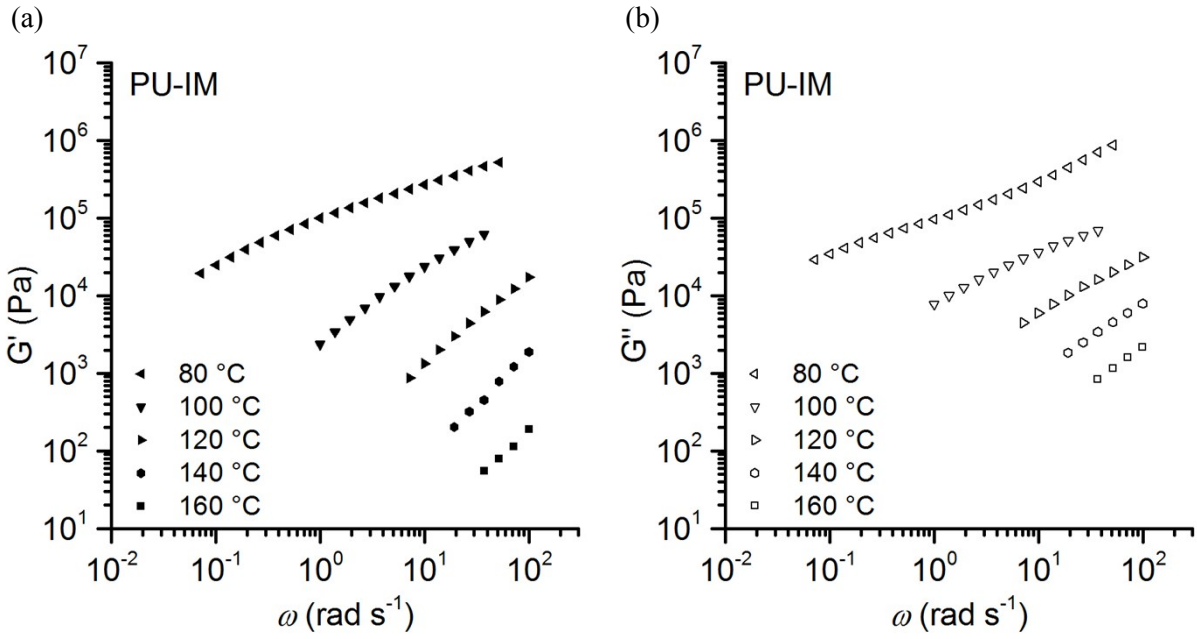

Figure S30: Frequency sweeps of (a) storage modulus (G′) and (b) loss modulus (G″) for PU-IM at varying temperature within the linear viscoelastic regime used for TTS plot in Figure 4c.

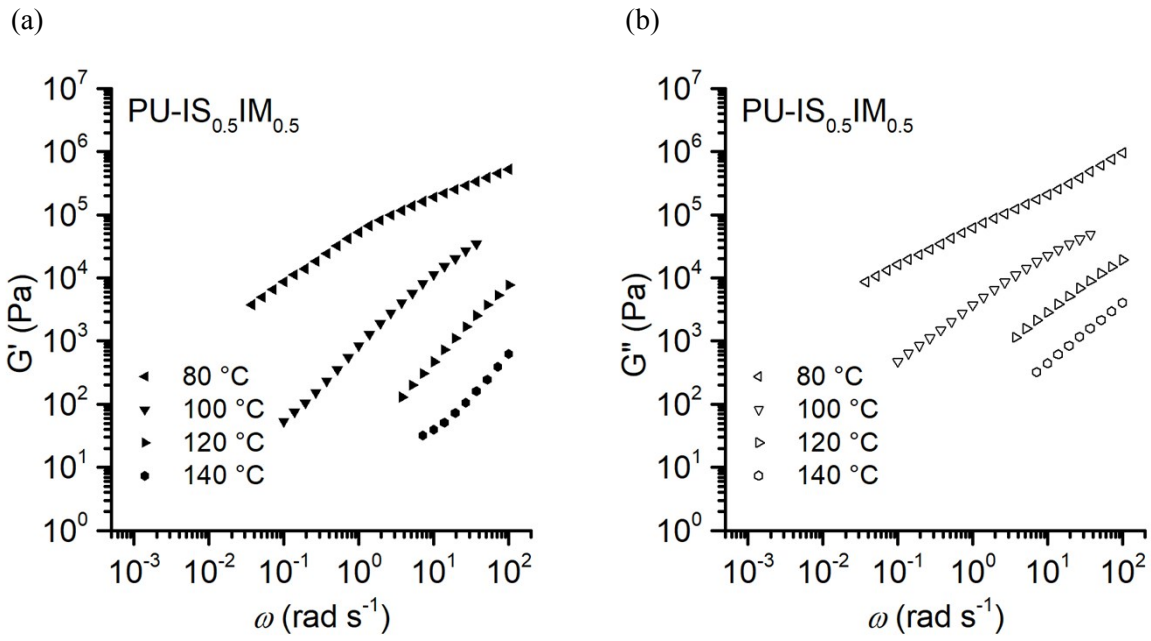

Figure S31: Frequency sweeps of (a) storage modulus (G′) and (b) loss modulus (G″) for PU-$IS_{0.5}IM_{0.5}$ at varying temperature within the linear viscoelastic regime used for TTS plot in Figure 4d.

Table S1: Strain values and shift factors (a_T) used for TTS master plots and WLF fitting.

Sample	T (ºC)	Strain (%)	a_T
PU-IS	70	0.05	600000
	80	0.1	7000
	90	0.5	500
	100	0.5	65
	120*	1	1
	140	1	0.175
PU-$IS_{0.5}IM_{0.5}$	80	1	1950
	100	1	20
	120*	1	1
	140	2	0.15
PU-IM	80	1	2000
	100	1	15
	120*	2	1
	140	2	0.1
	160	3	0.023

*reference temperature (T_{ref})

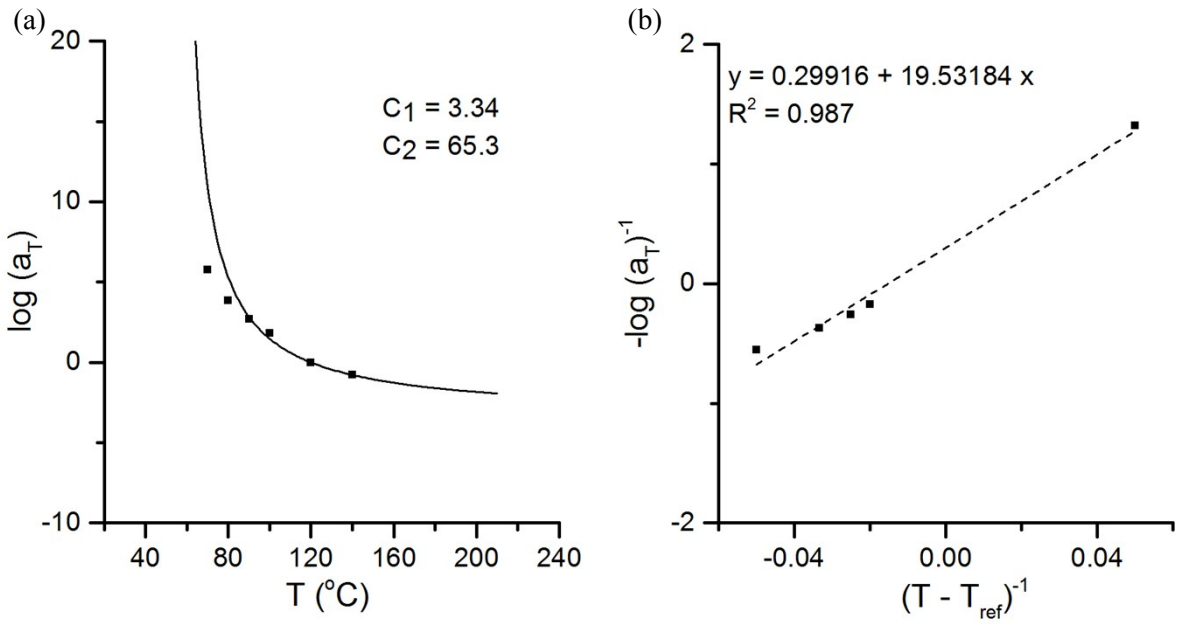

Figure S32: (a) Logarithmic shift factors for PU-IS vs *T* with T_{ref} = 120 ºC. Solid line is WLF equation using C_1 = 3.34 and C_2 = 65.3. (b) Linearized version of WLF equation plotting shift factors for PU-IS with T_{ref} = 120 ºC. C_1 is found by taking 1/y-intercept, and C_2 by taking slope × C_1

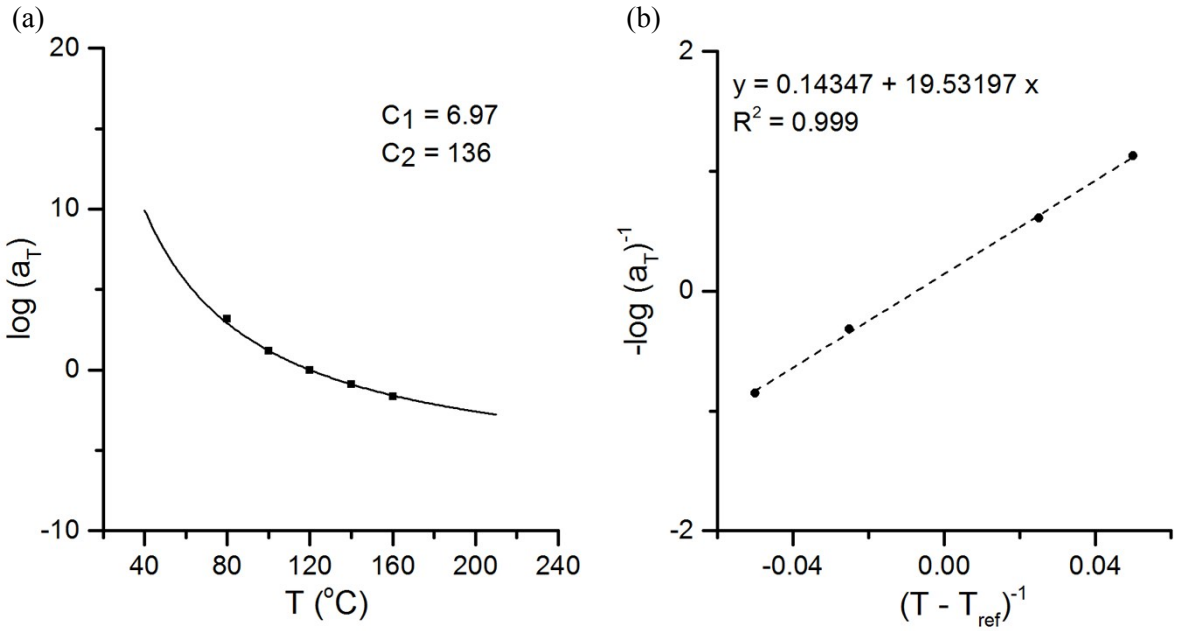

Figure S33: (a) Logarithmic shift factors for PU-IM vs *T* with T_{ref} = 120 ºC. Solid line is WLF equation using C_1 = 6.97 and C_2 = 136. Linearized version of WLF equation plotting shift factors for PU-IM with T_{ref} = 120 ºC. C_1 is found by taking 1/y-intercept, and C_2 by taking slope × C_1

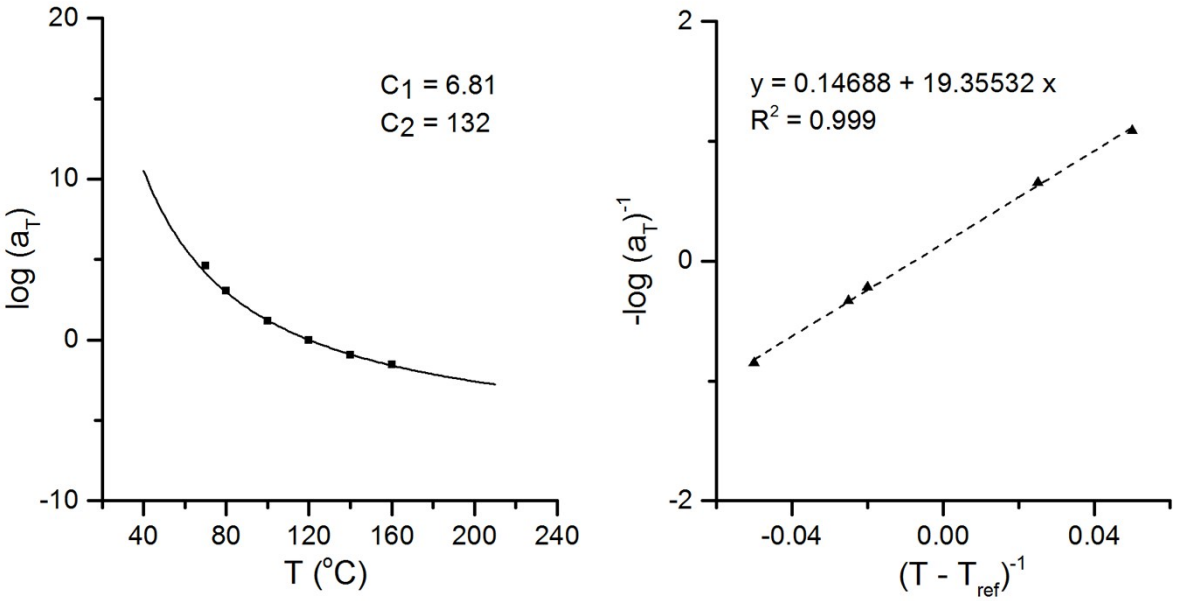

Figure S34: Logarithmic shift factors for PU-$IS_{0.5}IM_{0.5}$ vs *T* with T_{ref} = 120 ºC. Solid line is WLF equation using C_1 = 6.81 and C_2 = 132. Linearized version of WLF equation plotting shift factors for PU-$IS_{0.5}IM_{0.5}$ with T_{ref} = 120 ºC. C_1 is found by taking 1/y-intercept, and C_2 by taking slope $\times$ C_1

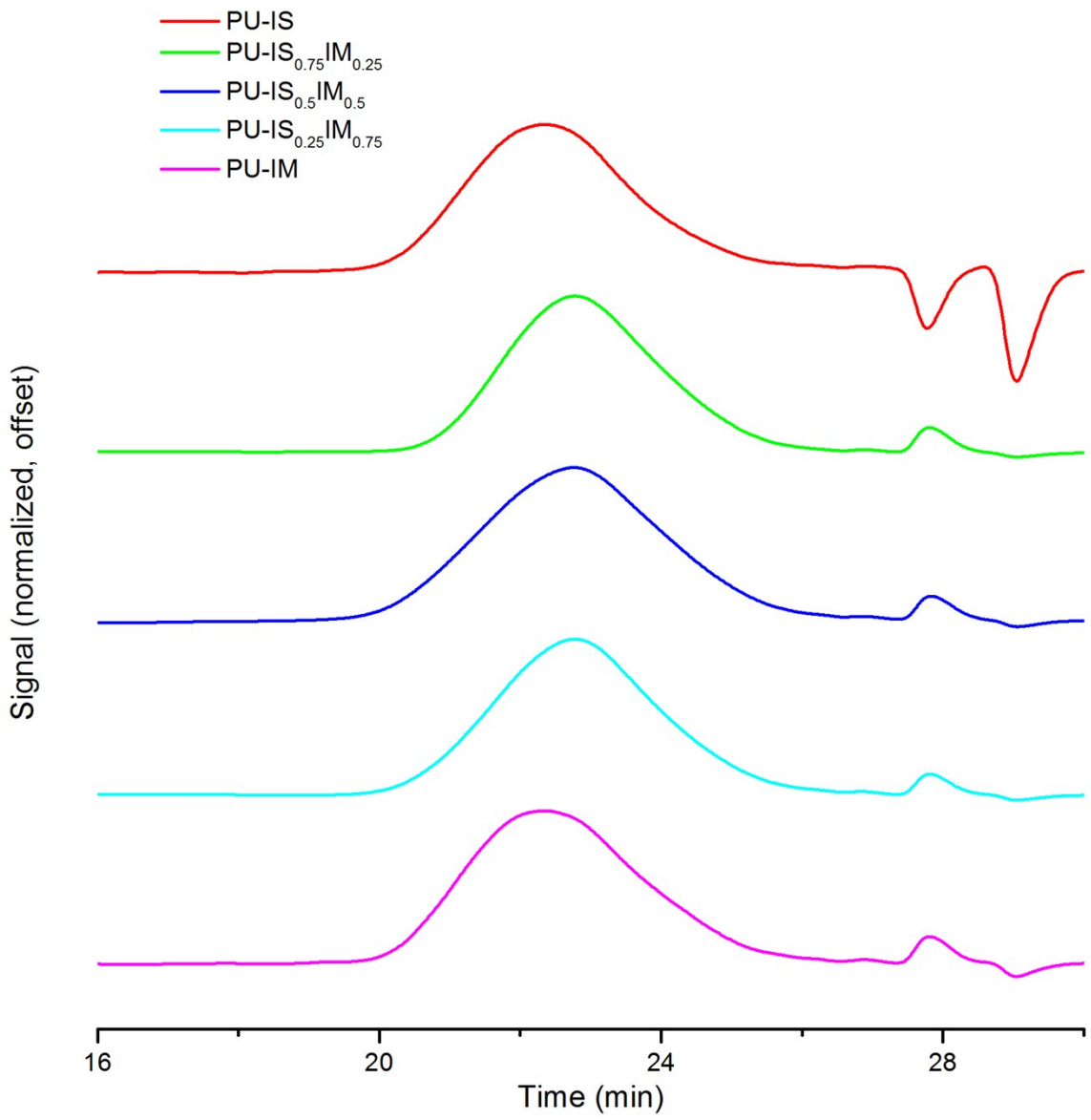

Figure S35: Normalized, offset, RI traces of polyurethanes obtained by SEC analysis. Samples were run at 25 ºC in DMF (0.05 M LiBr).

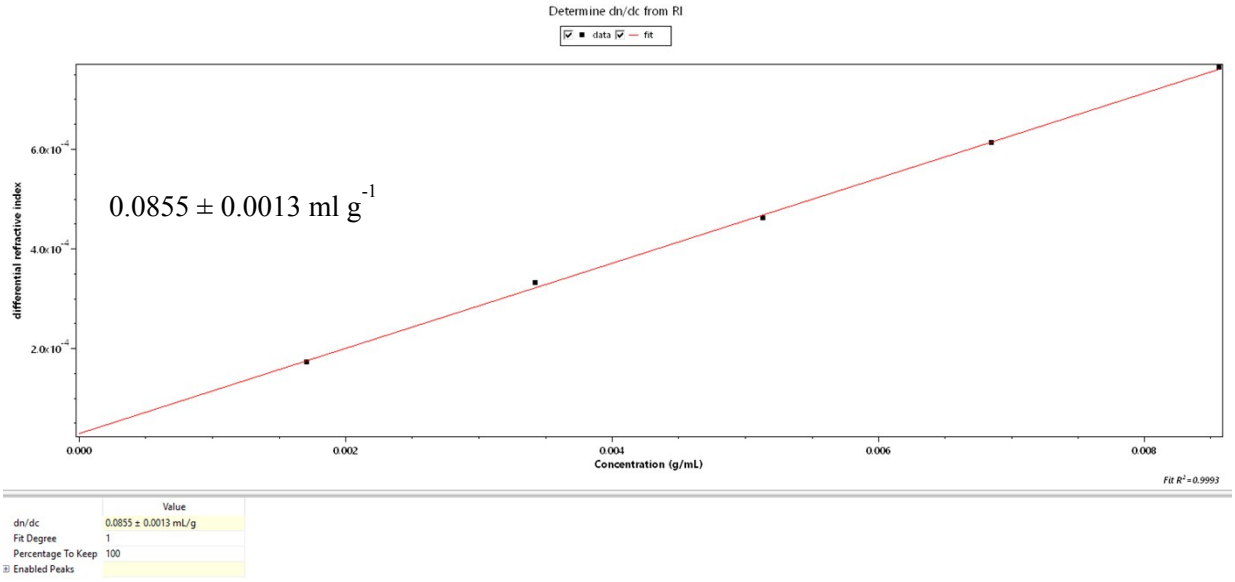

Figure S36: Linearized *dn*/*dc* determination for PU-IS obtained from RI detector generated by ASTRA software. Samples were dissolved in DMF (0.05 M LiBr stabilized) with known concentrations, and injected directly into the detector.

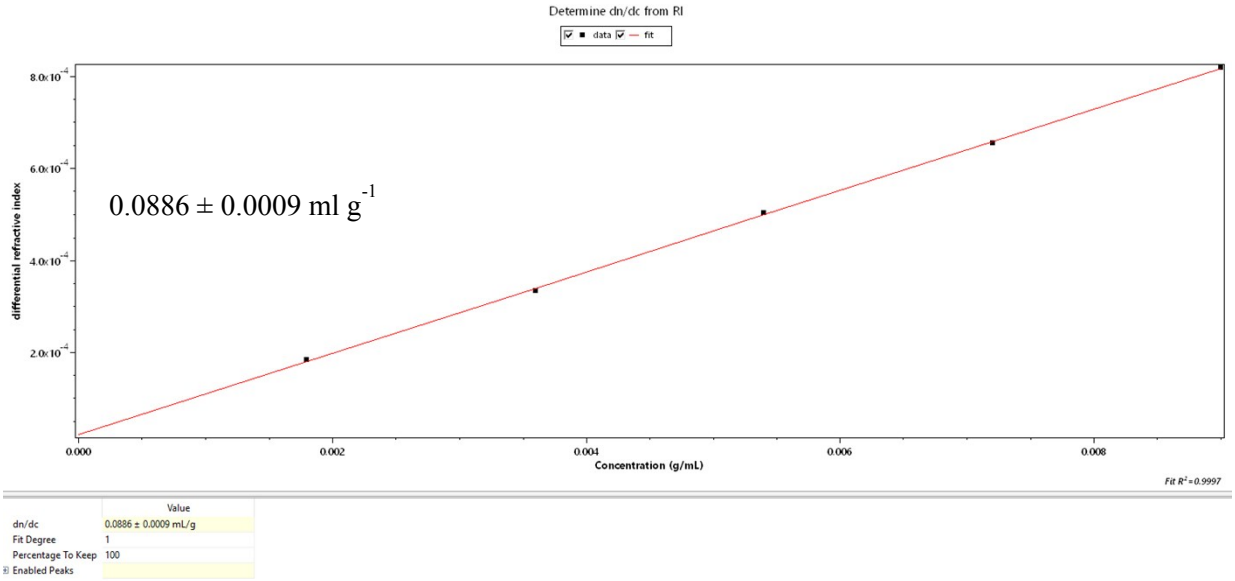

Figure S37: Linearized *dn*/*dc* determination for PU-IM obtained from RI detector generated by ASTRA software. Samples were dissolved in DMF (0.05 M LiBr stabilized) with known concentrations, and injected directly into the detector.

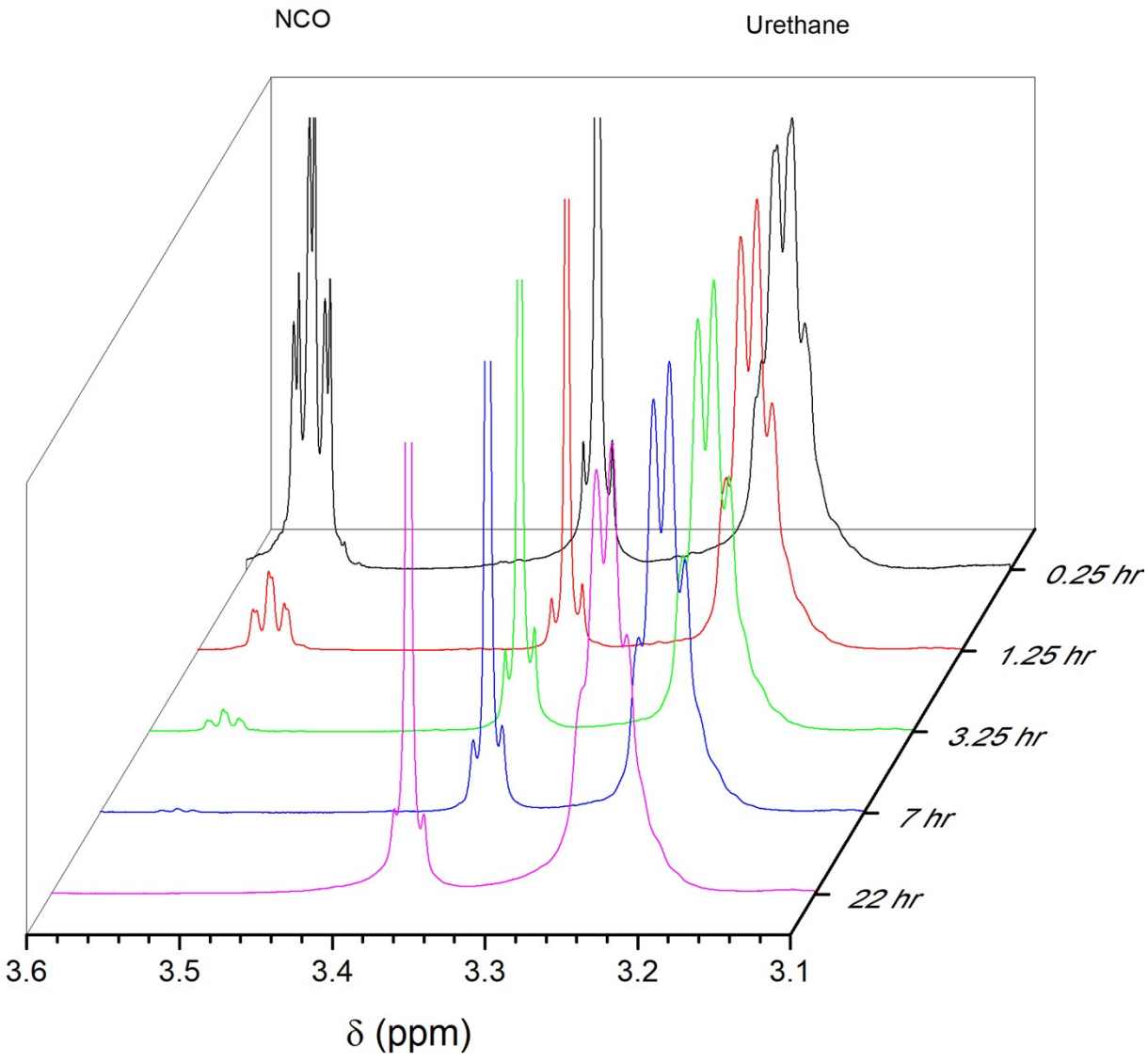

Figure S38: ^{1}H NMR time study of polymerization of ISBIP and BHMF, showing complete loss of the peak associated with the methylenes adjacent to the isocyanate at ~3.52 ppm.

Table S3: Polymerization conditions for each reported PU, showing the stoichiometric ratio of the monomers (r)

Sample	% Yield	mmol BHMF	mmol ISBIP/IMBIP	r
PU-IM	88	14.699	14.699	0.99997
PU-$IS_{0.25}IM_{0.75}$	66	11.803	11.804	0.99987
PU-$IS_{0.5}IM_{0.5}$	92	14.774	14.775	0.99993
PU-$IS_{0.75}IM_{0.25}$	82	14.763	14.765	0.99987

PU-IS	88	9.120	9.119	0.99996

REFERENCES

1. Van Krevelen, D. W.; Te Nijenhuis, K., *Properties of Polymers: Their Correlation with Chemical Structure; Their Numerical Estimation and Prediction from Additive Group Contributions*. Elsevier: 2009; p 1030.
2. Ganewatta, M. S.; Ding, W.; Rahman, M. A.; Yuan, L.; Wang, Z.; Hamidi, N.; Robertson, M. L.; Tang, C., Biobased Plastics and Elastomers from Renewable Rosin via "Living" Ring-Opening Metathesis Polymerization. *Macromolecules* **2016,** *49*, 7155-7164.